mathematics

MDPI

Article

Pricing Optimization for High-Speed Railway Considering Hybrid Choice Behavior of Heterogeneous Passengers Under Stochastic Demand

Yu Wang [1,3] and Zhendong Wang [2,3,*]

[1] 12306 Science and Technology Innovation Center, China Academy of Railway Sciences Corporation Limited, Beijing 100081, China; 23115087@bjtu.edu.cn
[2] Institute of Signal and Communication, China Academy of Railway Sciences Corporation Limited, Beijing 100081, China
[3] School of Traffic and Transportation, Beijing Jiaotong University, Beijing 100044, China
* Correspondence: 23115109@bjtu.edu.cn

Abstract

Passenger heterogeneity in loyalty fundamentally influences their choice behaviors, and is pivotal to railway differentiated pricing. Thus, travelers are categorized into loyal passengers and non-loyal passengers. According to the generalized cost minimization, we identify a train priority sequence reflecting consistent preferences of loyal passengers and establish a train selection probability model based on stochastic preferences of non-loyal passengers. Then, a hybrid choice model resulting from the distinct decision-making processes of these two passenger categories is formulated. A nonlinear pricing optimization model in the scenario of multiple train categories with multiple trains is established. An improved Particle Swarm Optimization algorithm based on the Sampling Fitness Strategy (SFS-PSO) is proposed to improve the solution accuracy. The SFS-PSO enhances the search diversity for the personal historical best positions and global best position without expanding the size of the particle swarm as much as possible. The case analysis demonstrates that the proposed pricing optimization approach can increase the expected revenue by 1.7%, validating the rationality of considering the hybrid choice behavior of passenger loyalty heterogeneity for the railway pricing optimization problem. Meanwhile, the case results highlighted the significant impact of the proportion of loyal passengers on revenue improvement.

Keywords: railway pricing optimization; passenger choice behavior; evolutionary algorithm; PSO; revenue management; loyal passenger; stochastic demand

MSC: 90B50; 91B24

check for updates

Academic Editors: Rui Zhong and Jun Yu

Received: 10 November 2025
Revised: 1 December 2025
Accepted: 3 December 2025
Published: 5 December 2025

Citation: Wang, Y.; Wang, Z. Pricing Optimization for High-Speed Railway Considering Hybrid Choice Behavior of Heterogeneous Passengers Under Stochastic Demand. *Mathematics* **2025**, *13*, 3897. https://doi.org/10.3390/math13243897

Copyright: © 2025 by the authors. Licensee MDPI, Basel, Switzerland. This article is an open access article distributed under the terms and conditions of the Creative Commons Attribution (CC BY) license (https://creativecommons.org/licenses/by/4.0/).

1. Introduction

1.1. Background

High-speed railway managers often set various prices for multiple trains according to their characteristics in China. Differentiated prices consciously guide passengers' decision-making, steering their choices toward achieving greater economic benefits for the high-speed railway. This strategy is known as differentiated pricing and is able to effectively improve the flexibility of railway prices [1]. Differentiated pricing is essentially a price discrimination strategy relying on understanding passengers' choice behavior.

1.1.1. Differentiated Pricing in Transportation

Many works of research investigated differentiated pricing strategies to achieve specific policy objectives. Li et al. [2] was one of the earlier scholars to introduce the differentiated pricing method to a railway system for management efficiency improvement. Hu et al. [3] assumed a competitive market environment containing all trains and flights between a long-distance origin–destination (OD) pair. They continued to propose a differentiated pricing approach for the high-speed railway to enhance its competitiveness. Cao et al. [4] classified train products on the basis of the station levels and the stop numbers, developing a differentiated pricing bi-objective comprehensive optimization model based on a multidimensional passenger flow assignment strategy. Qin et al. [5] divided the entire passenger group and used prospect theory to construct a differentiated pricing model under elastic demand. Shi et al. [6] believed that passengers will take into account multiple factors such as train routes, stop plans, ticket prices, seat availability, and departure times to choose trains. Then, a nonlinear optimization model integrating differentiated pricing and seat allocation for the high-speed railway is constructed. Jing et al. [7] established a differentiated pricing approach based on the multi-dimensional characteristics of trains. This model balanced the occupancy rates between trains. Zhang et al. [8] employed the passenger exchange coefficients in a differentiated pricing model for urban rail transit. Subsequently, the time-dependent differentiated pricing model greatly influenced dispersing passenger flow and ensured the safety of urban rail transit.

1.1.2. Passenger Classification

The fundamental basis of differentiated pricing lies in identifying, analyzing, and modeling passenger choice behaviors. Due to the passenger heterogeneity, the choice behaviors among passengers vary significantly. Therefore, it is reasonable to first divide passengers based on their heterogeneity reflected by preferences before modeling their choice behaviors. Yang et al. [9] proposed a two-step approach integrating Latent Class Analysis (LCA) with Random Parameter Logit (RPL) to quantify a variety of passengers' preferences for parallel trains. Chen et al. [10] used the Gaussian Mixture Model (GMM) to define four heterogeneous passenger groups in high-speed railway market, named as Price Sensitive (PS), General Business (GB), Peak-hours Enthusiastic (PE), and Leisure Experience (LE).

On the other hand, as an important measure of railway revenue management, market segmentation requires managers to categorize the entire railway market into submarkets according to the following two aspects: passenger-oriented and train-oriented [11]. Passenger-oriented market segmentation is just passenger classification in essence. In most cases, time and price are viewed as two major factors affecting passenger demands, and become the basis for passenger classification, such as time-sensitive passengers and price-sensitive passengers [12]. Moreover, income levels and consumption capacity [13], travel purpose [14], the number of tickets (the allowed number of rides) purchased at one time [15,16], advance ticket purchase time [17], and passenger loyalty [18] are also regarded as the main factors guiding passenger classification in other literature.

1.1.3. Passenger's Choice Behavior

A critical step in building models to address the optimization problem of management and operation in railways is the mathematically representation of choice behaviors for each passenger group. Yan et al. [19] constructed a conditional Logit model to analyze the influencing choice factors for business passengers and non-business passengers. Gao et al. [20] proposed a mixed Logit model to assess passengers' preferences in train choice through a systematic investigation under market segmentation. Qiu et al. [21] explored the factors

influencing passengers' choice based on the non-aggregate discrete selection theory. Hetrakul et al. [22] conducted an analysis using Internet booking data with limited individual variables to investigate the heterogeneous characteristics of passenger behaviors under different distances. Wang et al. [23] established an optimization model that considered the choice processes of existing passengers and incremental passengers, respectively.

1.1.4. Loyal Passenger

Loyal passengers refer to those who exhibit a certain degree of preference for a specific mode of transportation [24] (taxi, bus, railway, and aviation) or for a certain type product of a transportation mode. They prioritize this type of product, thereby demonstrating high loyalty to it. Characterized by strong travel stickiness, high economic value, and a low churn rate, loyal passengers are key targets for marketing and service efforts for transportation enterprises.

Most existing studies on loyal passengers focused on the factors affecting passenger loyalty or how to evaluate passenger loyalty. Li et al. [25] studied the relationships between service quality, information collection, switching costs, attraction of alternatives, and passenger loyalty. The outcomes suggested that service quality proportional to passenger satisfaction is the most important factor influencing passenger loyalty in public transportation. The same conclusion was also reached in the literature [26,27]. Akbari et al. [28] proposed a generalized ordered Logit model which is an improvement on the Multinomial Logit model (MNL) to test passenger loyalty. Wong et al. [29] developed a method to assess passenger loyalty based on a data-mining technique. They found that loyal passengers had obvious preferences. Saisrikanta et al. [30] adopted a variety of machine-learning techniques to predict passenger loyalty to help airline companies recognize a loyal customer group. Chacon et al. [31] discussed passenger buying behavior within the airline industry and revealed the relationships between the loyal passenger groups and individual characteristics of passengers. They suggested that latent loyal passengers could be converted into fully loyal passengers. Gu et al. [32] took account of the effects of mode similarity and heterogeneity on decision-making, using a nested weibit model to explore the choice behaviors of passengers who are not loyal to customized bus services.

A limited amount of literature discussed how to apply appropriate mathematical forms to model the issue of the choice behaviors of loyal passengers in optimization. Lu et al. [33] established a timetable optimization model through modeling the choice behavior of airport loyal passengers to the bus service. Zhu et al. [34] proposed a dynamic tickets pricing model considering the differences in selection between loyal passengers and ordinary passengers on booking seats. Zhang et al. [35] categorized the passengers according to whether they have loyalty to online direct sales of airlines. Then, the decision-making processes of these two passenger groups were modeled and a pricing optimization model to determine the choice between online direct sales and distribution channels was proposed.

1.2. Limitations of Existing Studies and Contributions

Although numerous studies explored passenger heterogeneity from various perspectives, most focused primarily on passenger classification based on heterogeneity [9,10,12–18]. The discussion on how to model the various choice behaviors reflected by differentiated decision-making processes based on passenger classification to optimize the price strategy remains inadequate.

Furthermore, some research recognized the differences in passenger choice behaviors, adopting the LCA [9] or the Logit-type model [19,20,28,29,32] to calculate the choice probabilities of various passenger groups based on utility maximization. While, in these models, a uniform mathematical construction is used to model the decision-making processes of

various passengers by giving different parameter values in the same form of choice function, this kind of approach fails to adequately capture the differences in the priorities and weights of factors affecting passenger choice behaviors among multiple passenger groups. Therefore, we believe that heterogeneous passengers exhibit a hybrid choice behavior composed of multiple distinct decision-making processes where different passenger categories demonstrate variations in preferences, choice objects, calculation frameworks for selection probability, and opt-out conditions. In addition, from the perspective of passengers, generalized cost minimization is a more suitable rule than utility maximization.

Although numerous studies [25–30] examined the role of loyal passengers in transportation operations, most of them focused on either identifying factors influencing passenger loyalty or developing methods to evaluate passenger loyalty, while relatively limited research [34] investigated modeling the choice behaviors of loyal passengers to inform pricing strategies.

As a result, this article proposes an optimization approach based on modeling the hybrid choice behavior of heterogeneous passengers under stochastic passenger flow. The main contributions are included as follows:

- This paper identifies a train priority sequence reflecting the consistent preferences of loyal passengers and constructs a train selection probability model with the stochastic preferences of non-loyal passengers.
- We develop a differentiated pricing optimization approach with a hybrid choice model consisting of multiple passenger decision-making processes under stochastic passenger flow.
- We regard both time value and cost expectation as random variables. This overcomes the limitation of treating them as constants in most previous studies, thus better aligning with reality. Then, a double integral considering both the time value and cost expectation as random variables is constructed to estimate the choice probabilities of non-loyal passengers.
- We propose an improved PSO algorithm based on a sampling fitness strategy (SFS-PSO) to enhance the search efficiency and accuracy in solving the nonlinear optimization model by optimizing the personal historical best position and global best position in certain steps of the iterative process.

This paper is organized as follows: Section 2 models the decision-making processes of loyal passengers and non-loyal passengers, respectively; Section 3 constructs a nonlinear pricing optimization model; Section 4 details the SFS-PSO algorithm; Section 5 states the numerical experiments; and Section 6 concludes the paper. Figure 1 describes the main research path.

1.3. Assumptions and Notations

The following reasonable assumptions are made based on actual operations;

(1) Referring to the literature [12], passengers are most sensitive to time and fares; thus, the generalized cost mainly takes into account the price and travel time.
(2) We only consider the second-class seat in the case analysis.
(3) All passengers are divided into two categories: business passengers and ordinary passengers [13,19].

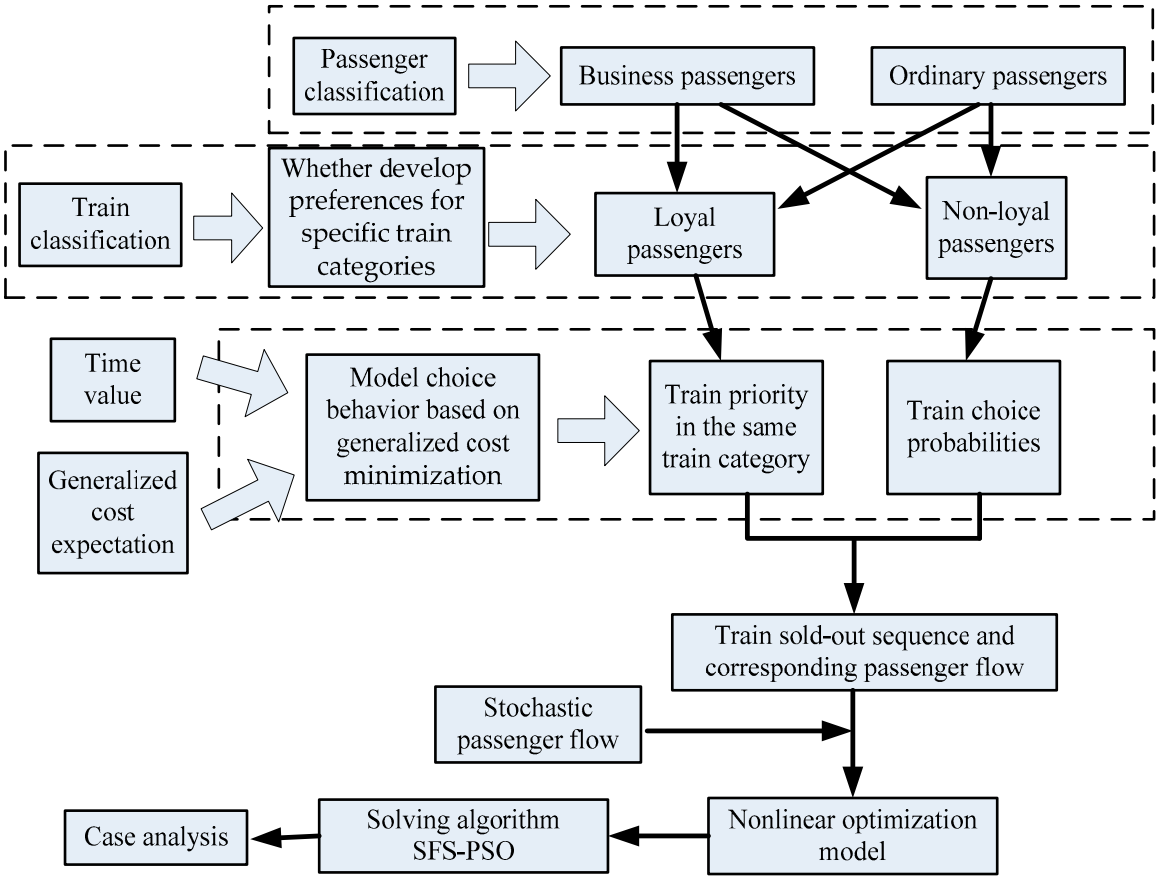

Figure 1. The proposed conceptual framework.

The variables, parameters, and sets are shown in Table 1.

Table 1. Notation.

Symbol	Variable	Unit
$d, i, \hat{d}$	Train category.	/
$k^d, q^i, \hat{k}^{\hat{d}}$	Train $k(q)$ belonging to train category $d(i)$. It also represents the priority of train $k(q)$ in train category $d(i)$.	/
j	Passenger category, including business passengers and ordinary passengers.	
u	Individual passenger.	/
P_j^d	Proportion of loyal passengers in passenger category j to train category d.	%
t_k^d	Travel time of train k belonging to train category d.	Min
v	Time value.	CNY/min
f	Generalized cost.	CNY
c_k^d	Number of tickets of train k belonging to train category d.	/
m_j	Proportion of passenger category j in total passengers.	%
$x_k^d, \overline{x}_k^d$	The corresponding passenger flow when the tickets of train k belonging to train category d are exactly sold out.	Passengers

Table 1. *Cont.*

Symbol	Variable	Unit
s_k^d	The purchase volume of tickets for loyal passengers upon the train k being sold out.	Passengers
g, w	Train ranking based on the sell-out sequence of trains.	/
$h_{k,g}^d$	Passenger flow when the tickets of train k in train category d with ranking g are sold out.	Passengers
R_g	Expected revenue under the situation g of stochastic demand.	CNY
	Parameter and set	
w_j	Coefficient of time value of non-loyal passengers in passenger category j.	/
$\overline{\omega}_j$	Coefficient of generalized cost expectation of non-loyal passengers in passenger category j.	/
K^d	Train set of train category d.	/
Z	Current discrete price set.	/
Symbol	**Decision Variable**	**Unit**
p_q^i	Price of train q belonging to train category i.	CNY

2. Modeling the Choice Behaviors of Loyal Passengers and Non-Loyal Passengers

The literature [36] reveals that the generalized cost incurred during trips can be relatively clearly perceived by passengers and guide their choices. Next, the differentiated choice models for loyal passengers and non-loyal passengers based on generalized cost minimization are separately constructed.

2.1. Loyal Passenger Identification

A product can be further subdivided into multiple categories on the basis of variations in functions and attributes. Due to the influence of various factors (such as consumption habits, individual experiences, and product awareness), consumers naturally develop preferences for a specific category of the product. For instance, when purchasing cars, people often exhibit brand preferences [37]. Consumers with high financial means may favor premium brands like Mercedes-Benz or BMW, and they are unlikely to opt for a Toyota car solely because of its lower price. Here, Mercedes-Benz and BMW constitute the premium car category, and affluent consumers typically limit their choices to the category. The above consumers are defined as loyal customers to the premium car category.

Similarly, a number of trains providing travel service between the same OD pair can also be subdivided into multiple train categories. A passenger who has a clear preference for a particular train category and consistently selects trains from the category in most cases is defined as a loyal passenger to that train category.

A passenger u belonging to passenger category j completes N_u journeys over a period of time, where n_u^d trips are on trains of category d. The total number of train trips taken by passenger u satisfies the following formula:

$$\sum_d n_u^d = N_u, \forall u \in j \tag{1}$$

Accordingly, whether passenger u is a loyal passenger of train category j can be determined by Formula (2) where η^d is the threshold:

$$\frac{n_u^d}{N_u} \geq \eta^d, \forall u \in j \tag{2}$$

2.2. Decision-Making Process of Loyal Passengers Based on Generalized Cost Minimization

Set α_j^d as a 0–1 variable. If passenger category j contains loyal passengers to train category d, then $\alpha_j^d = 1$; otherwise, $\alpha_j^d = 0$. Let $d = 0$ represents the largest train category composed of all trains. Note that there are no loyal passengers to train category $d = 0$ and $\alpha_j^0 = 0, \forall j$. For any passenger category j, the proportions of loyal passengers to all train categories sum to 1.

$$\sum_d P_j^d \bullet \alpha_j^d = 1, \ \forall j \tag{3}$$

Most passengers mainly focus on two factors, product attributes including departure time, travel time, comfort, and safety, alongside the price, when choosing a train. According to the survey results from the literature [36], the product attributes of trains in the same category exhibit minimal differentiation that loyal passengers perceive no distinction between them, making the trains substitutable excluding the price factor. As a result, the generalized cost depends only on the prices from the perspective of loyal passengers. Loyal passengers will choose the one with the currently lowest price from the preferred train category, forming a price-dependent priority sequence for all trains in the same category. If the tickets of the highest-priority train are sold out, loyal passengers will turn to opt for the next-priority train. The demand from loyal passengers sequentially shifts within the preferred train category until no tickets are available for sales. Evidently, this means a definite choice probability with 100%. Loyal passengers sequentially select trains until all tickets of the trains in the same category are fully booked. Then, they have to give up high-speed railway trips.

Therefore, loyal passengers possess consistent preferences and exhibit significantly lower probabilities of giving up compared to non-loyal passengers, making them key marketing targets for railway enterprises. By optimizing pricing strategies to prevent tickets from being entirely purchased by non-loyal passengers to provide loyal passengers with more preferred trains to choose, high-speed railway enterprises can further cultivate more loyal passengers for long-term revenue, aligning with the principles of revenue management and marketing requirements. The decision-making process of loyal passengers is illustrated in Figure 2.

2.3. Decision-Making Process of Non-Loyal Passengers Based on Generalized Cost Minimization

Non-loyal passengers have no definite preference for specific train category and the generalized costs are primarily affected by the ticket price and travel time [12]. Therefore, the generalized cost of selecting train k in train category d is given as $f_k^d(v_j)$ which can be computed by Equation (4):

$$f_k^d(v_j) = p_k^d + v_j \bullet t_k^d \tag{4}$$

To address the limitation of treating the time value as a constant, it is assumed that the time value v_j follows an exponential probability distribution (Figure 3a). Empirical observations indicate that a minority of the people earn high incomes, resulting in higher time values and a higher cost expectation, whereas the majority of the people have lower incomes and, consequently, smaller time values and cost expectation. That is to say, the probability is big for a low time value and small for a high time value, with the probability decreasing as the time value increases. This characteristic can be described by

the exponential distribution. Thus, the exponential distribution for the time value and cost expectation is adopted. The probability density function of the time value is given by Equation (5) where $v_{0,j}$ is the minimum time value:

$$CF(v_j) = \begin{cases} \omega_j \bullet \exp[-\omega_j \bullet (v_j - v_{0,j})], v_j \geq v_{0,j} \\ 0, v_j < v_{0,j} \end{cases} \quad (5)$$

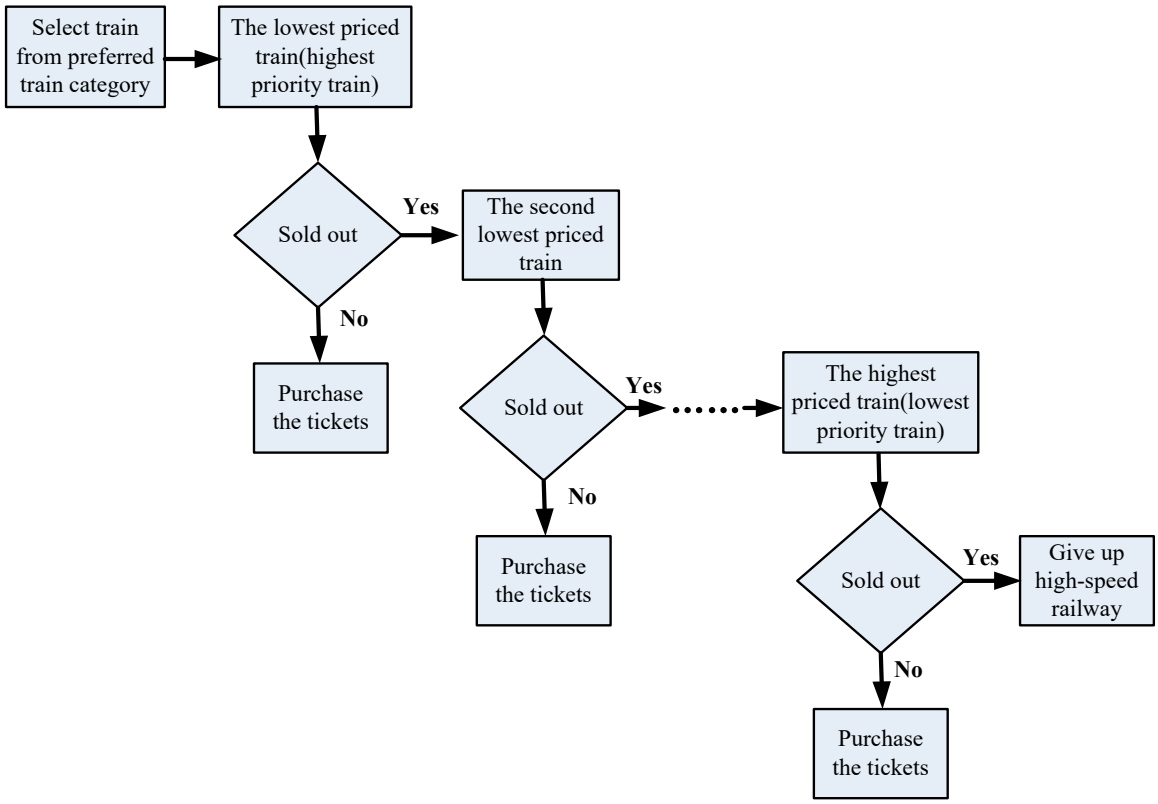

Figure 2. The decision-making process of loyal passengers.

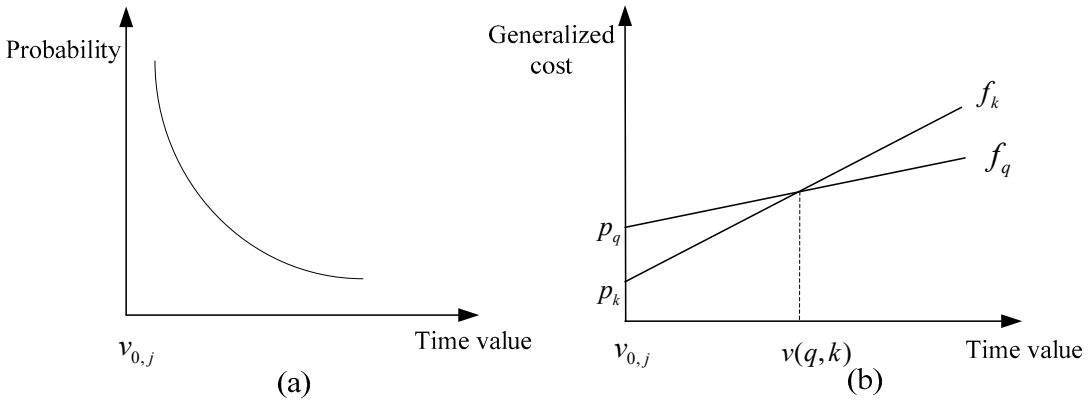

Figure 3. (**a**) Probability density function of time value. (**b**) The relationship between time value and selected train.

Figure 3b illustrates the relationship between the time value and selected train. $v(q,k)$ expresses the balance point of trains k and q. If $v_j > v(q,k)$, the generalized cost of train k is higher than that of train q; then, passengers naturally select train k. In contrast, passengers choose train k when $v_j < v(q,k)$.

However, the non-loyal passengers may reject the high-speed railway when the generalized cost of the train to be selected exceeds their expectation. Resembling the distribution characteristics of the time value, assume the cost expectation of the non-loyal passengers obey an exponential probability distribution in Formula (6) where $f_{0,j}$ stands for the lower limit of the generalized cost expectation for passenger category j.

$$CF(f_j) = \begin{cases} \overline{\omega}_j \bullet \exp[-\overline{\omega}_j \bullet (f_j - f_{0,j})], f_j \geq f_{0,j} \\ 0, f_j < f_{0,j} \end{cases} \tag{6}$$

Due to the independence of time value v_j and generalized cost expectation $f_{0,j}$, $Pb_{k,j}^d$ is formulated by Equation (7) to measure the probability of choosing train k for passenger category j:

$$Pb_{k,j}^d = \int_{v(k-1,k)}^{v(k,k+1)} CF(v_j) \int_{f_k^d(v_j)}^{+\infty} CF(f_j) df_j dv_j \tag{7}$$

where the domain $[v(k, k+1), v(k-1, k)]$ of the outer definite integral is determined by generalized cost minimization which is illustrated in Figure 3b; that is, the generalized cost of train k is minimal when the time value ranges between domain $[v(k, k+1), v(k-1, k)]$. As a result, passengers will select train k. The domain $[f_k^d(v_j), +\infty]$ of the inner indefinite integral ensures the generalized cost expectation must be higher than the actual generalized cost of train k. Due to the fact that $f_k^d(v_j)$ is a function with v_j, Equation (7) integrates the time value with the generalized cost expectation to estimate the probability of selecting train k.

2.4. Passenger Flow and Ticketing Process

Under stochastic passenger flow, various passenger flow volumes lead to varying situations of trains being sold out, which, in turn, directly change the choice of loyal passengers. It is necessary to first calculate the thresholds of passenger flow volumes corresponding to each sell-out situation, which divide the stochastic passenger flow into multiple probability events.

With the progress of ticket sales during the pre-sale period, loyal passengers must be able to purchase the tickets of the train with the highest priority $k = 1$ in each train category. m_j symbolizes the proportion of passenger category j in total passengers. Let $u_j^d = m_j \bullet P_j^d \bullet \alpha_j^d$, and the number of tickets purchased by loyal passengers upon the highest-priority train $k = 1$ being sold out is s_1^d. At this time, the corresponding passenger flow x_1^d can be obtained by Formula (8):

$$\begin{aligned} c_1^d &= x_1^d \bullet \sum_{j \in J} (u_j^d + u_j^0 \bullet Pb_{k,j}^d) \\ \Rightarrow x_1^d &= \frac{c_1^d}{\sum_{j \in J} (u_j^d + u_j^0 \bullet Pb_{k,j}^d)} \end{aligned} \tag{8}$$

$$s_1^d = x_1^d \bullet \sum_{j \in J} u_j^d \tag{9}$$

where $c_1^d = x_1^d \bullet \sum_{j \in J} (u_j^d + u_j^0 \bullet Pb_{k,j}^d)$ indicates that the passenger flow is equal to the number of tickets allocated when train $k = 1$ is just sold out. With the passenger flow growing, the tickets of any train $k, \forall k > 1$ being exactly sold out triggers the following two scenarios:

(1) Scenario 1: Loyal passengers have secured tickets for train k. The following Equations (10) and (11) for x_k^d and s_k^d are developed:

$$\begin{aligned} c_k^d &= x_k^d \bullet (\sum_{j \in J} u_j^d + u_j^0 \bullet Pb_{k,j}^d) - \sum_{q=1}^{k-1} s_q^d \\ \Rightarrow x_k^d &= \frac{c_k^d + \sum_{q=1}^{k-1} s_q^d}{\sum_{j \in J} u_j^d + u_j^0 \bullet Pb_{k,j}^d} \end{aligned} \tag{10}$$

$$s_k^d = x_k^d \bullet \sum_{j \in J} u_j^d - \sum_{q=1}^{k-1} s_q^d \tag{11}$$

(2) Scenario 2: Loyal passengers fail to obtain any tickets for train k. All tickets for train k have been purchased by non-loyal passengers in advance. The corresponding passenger flow is recorded as $\overline{x}_k^d$ at this moment:

$$\begin{aligned} c_k^d &= \overline{x}_k^d \bullet \sum_{j \in J} u_j^0 \bullet Pb_{k,j}^d \\ \Rightarrow \overline{x}_k^d &= \frac{c_k^d}{\sum_{j \in J} u_j^0 \bullet Pb_{k,j}^d} \end{aligned} \tag{12}$$

Obviously, Scenario 1 and Scenario 2 are two mutually exclusive events where tickets for train k are either entirely purchased by non-loyal passengers (Scenario 2) or concurrently purchased by both loyal passengers and non-loyal passengers (Scenario 1). In other words, only one of x_k^d or $\overline{x}_k^d$ can exist. To judge which scenario occurs, the corresponding passenger flow x_k^d of each train is computed and x_k^d of every two adjacent trains in the sequence are compared. As a result, the following two propositions are proposed to facilitate a better understanding of the judging process for the reviewers.

Proposition 1. *For any train category d, if loyal passengers have purchased tickets for train k, then all trains in the same category with priorities higher than train k must have already sold out tickets (logical proof).*

Proposition 1 can be mathematically expressed by Formula (13);

$$x_k^d \neq \varnothing \Rightarrow x_k^d > \max(x_q^d), \forall q < k, \forall q \in K^d \tag{13}$$

The proof for Proposition 1 follows a straightforward logical derivation, where $q < k$ expresses train q is assigned a higher priority than train k. $x_k^d \neq \varnothing$ means Scenario 1 happens where loyal passengers successfully buy tickets for train k.

Proposition 2. *If x_k^d is less than x_q^d (the priority of train q is immediately before that of train k), then no loyal passengers are able to purchase tickets for train k.*

Proposition 2 can be mathematically expressed by the following formula:

$$x_k^d \leq \max(x_q^d), \forall q < k, \forall q \in K^d \Rightarrow x_k^d = \varnothing \tag{14}$$

Proposition 2 demonstrates that, for any two trains k and q, if the passenger flow x_k^d corresponding to the higher-priority train k being sold out is smaller than x_q^d of the lower-priority train q, all tickets for train k have been purchased by non-loyal passengers in advance. Thus, loyal passengers fail to buy tickets for train k and there only exists $\overline{x}_k^d$.

Therefore, by sequentially comparing x_k^d and $x_q^d, \forall q < k, \forall q \in K^d$ according to Proposition 2, whether loyal passengers are able to purchase tickets for a given train k (equal to whether Scenario 2 holds) is confirmed.

Proposition 2 is the inverse negation of Proposition 1. If Proposition 2 holds, then Proposition 1 must also hold. h_k^d, which stands for the final passenger flow when train k is exactly sold out regardless of which scenario happens, is obtained.

$$h_k^d = \begin{cases} x_k^d, x_k^d \neq \varnothing \\ \overline{x}_k^d, x_k^d = \varnothing \end{cases} \tag{15}$$

All trains are sorted by the passenger flow h_k^d of each train, resulting in a sequence that satisfies Equation (16) where g_k means train k ranks g in the ticket sold-out sequence among all trains:

$$g_k > w_q \Leftrightarrow h_{k,g}^d > h_{q,w}^i, \forall k \in K^d, \forall q \in K^i \tag{16}$$

Finally, the sequence of all sold-out trains and the corresponding passenger flow $h_{k,g}^d$ is derived.

3. Mathematical Model

3.1. Expected Revenue

According to the literature [38], the total passenger flow x follows a truncated normal probability distribution, $x \sim N(\mu, \sigma)$:

$$f(x) = \frac{1}{\sqrt{2\pi}\sigma} \bullet \exp\left(-\frac{(x-\mu)^2}{2\sigma^2}\right), x > 0 \tag{17}$$

The stochastic passenger flow x is divided into $\max(g)+1$ situations according to each $h_{k,g}^d$ used as the bound value for the probabilistic integration (see Formula (21)). Under any situation $g, g = 0, 1, 2 \ldots \max(g)$, the corresponding total passenger flow interval can be written as $(h_{k,g}^d, h_{\hat{k},g+1}^{\hat{d}}]$. $h_{k,g}^d$ represents the passenger flow of train k belonging to category d with ranking g in the sold-out sequence. $h_{\hat{k},g+1}^{\hat{d}}$ denotes the passenger flow of train $\hat{k}$ in category $\hat{d}$ with ranking $g+1$ in the sold-out sequence. Formulate equation $h_{k=0,0}^d = 0$ where $k = 0$ represents a virtual train with a total passenger flow volume of zero to unify the equation expression under diverse passenger flow situations.

Due to the fact that ticket sales for different trains proceed simultaneously and passengers' selection probabilities across different trains vary, it is inevitable that tickets of some trains are sold out while the others remain available. The 0–1 variables $\theta_{k,q}^{d,i}$ and $\beta_{k,q}^{d,i}$ to describe the relationship between trains in terms of their sold-out sequence are introduced by Formulae (18) and (19), respectively. If train k^d is sold out before train q^i, then $\theta_{k,q}^{d,i} = 1$; otherwise, $\theta_{k,q}^{d,i} = 0$. Similarly, when train k has the highest-priority among all unsold-out trains in category d under the total passenger flow $h_{q,g}^i$, then $\beta_{k,q}^{d,i} = 1$; otherwise, $\beta_{k,q}^{d,i} = 0$. Constraint (20) ensures that there is only one highest-priority train in any train category:

$$\theta_{k,q}^{d,i} = \begin{cases} 1, h_{k,g}^d \leq h_{q,\hat{g}}^i \\ 0, otherwise \end{cases} \tag{18}$$

$$\beta_{k,q}^{d,i} = \begin{cases} 1, h_{k,g}^d = \min(h_{\hat{k},\hat{g}}^d) | \theta_{\hat{k},q}^{d,i} = 0, \forall \hat{k}, \forall \hat{g} \\ 0, otherwise \end{cases} \tag{19}$$

$$\sum_{q \in K^i} \beta_{q,k}^{i,d} \bullet (1 - \theta_{q,k}^{i,d}) = 1, \forall i \tag{20}$$

The total expected revenue consists of three components under a given total passenger flow: (1) the expected revenue from sold-out trains, in which tickets are purchased by both loyal passengers and non-loyal passengers; (2) the expected revenue from loyal passengers purchasing tickets for trains that have not been sold out; and (3) the expected revenue from non-loyal passengers purchasing tickets for trains that have not been sold out.

For situation $g = 1, 2, \ldots \max(g)$, the expected revenue can be computed by Equations (21)–(24):

(1) The expected revenue from sold-out trains $\hat{R}_g$ is computed by Formula (21), where the passenger flow x between $(h_{k,g}^d, h_{\hat{k},g+1}^{\hat{d}}]$ means train k is already sold out. $i|i \neq 0$ denotes the exclusion of the largest train category formed by all train set. $\sum_{i|i\neq 0} \sum_{q \in K^i}$ means the iterate over all trains in all train categories. For any train q in train category i, if $\theta_{q,k}^{i,d} = 1$, this indicates train q is sold out. Thus, the total expected revenue from sold-out trains consists of the expected revenue of train q:

$$\hat{R}_g = \int_{h_{k,g}^d}^{h_{\hat{k},g+1}^{\hat{d}}} \sum_{i|i\neq 0} \sum_{q \in K^i} \theta_{q,k}^{i,d} \bullet c_q^i \bullet p_q^i \bullet f(x) dx \tag{21}$$

(2) The expected revenue $\widetilde{R}_g$ is generated by loyal passengers purchasing tickets for trains that have not been sold out in Formula (22), where $\theta_{q,k}^{i,d} = 0$ and $\beta_{q,k}^{i,d} = 1$ mean train q is not sold out and has the highest-priority among all unsold-out trains in its category d. Thus, the passengers with the amount of $x - h_{q,g}^i$ will purchase the tickets of all unsold-out trains (including train q). Due to the fact that train q possesses the highest-priority among all unsold-out trains in its category, a portion of its tickets must have been purchased by loyal passengers. At this time, the total expected revenue comprises the expected revenue generated by loyal passengers from unsold-out train q.

$$\widetilde{R}_g = \int_{h_{k,g}^d}^{h_{\hat{k},g+1}^{\hat{d}}} (x - h_{k,g}^d) \bullet \sum_{i|i\neq 0} \sum_{q \in K^i} \sum_j u_j^i \bullet \beta_{q,k}^{i,d} \bullet (1 - \theta_{q,k}^{i,d}) \bullet p_q^i \bullet f(x) dx \tag{22}$$

(3) The expected revenue $\overline{R}_g$ comes from non-loyal passengers purchasing tickets of unsold-out trains in Formula (23), where the passenger flow x between $(h_{k,g}^d, h_{\hat{k},g+1}^{\hat{d}}]$ means that train k is already sold out, whereas the adjacent train $\hat{k}$ is not sold out. If $\theta_{q,k}^{i,d} = 0$, this indicates the train q is certainly not sold out. Since the preferences of non-loyal passengers are not homogeneous, the tickets of train q must be purchased by non-loyal passengers with a certain probability to yield the revenue:

$$\overline{R}_g = \int_{h_{k,g}^d}^{h_{\hat{k},g+1}^{\hat{d}}} x \bullet \sum_{i|i\neq 0} \sum_{q \in K^i} \sum_j u_j^0 \bullet Pb_{q,j}^i \bullet (1 - \theta_{q,k}^{i,d}) \bullet p_q^i \bullet f(x) dx \tag{23}$$

Consequently, the total expected revenue of situation g amounts to R_g, including the above three expected revenues:

$$R_g = \hat{R}_g + \widetilde{R}_g + \overline{R}_g = \int_{h^d_{k,g}}^{\hat{h^d_{k,g+1}}} [\sum_{i|i\neq 0} \sum_{q\in K^i} \theta^{i,d}_{q,k} \bullet c^i_q + (x - h^d_{k,g}) \bullet \sum_{i|i\neq 0} \sum_{q\in K^i} \sum_j u^i_j \bullet \beta^{i,d}_{q,k} \bullet (1 - \theta^{i,d}_{q,k}) + x \bullet \sum_{i,i\neq 0} \sum_{q\in K^i} \sum_j u^0_j \bullet Pb^i_{q,j} \bullet (1 - \theta^{i,d}_{q,k})] \bullet p^i_q \bullet f(x)dx \quad (24)$$

Once all tickets are sold out, the total expected revenue remains unchanged regardless of any growth in total passenger flow. This is the last situation, $\max(g) + 1$. Thus, let $h_{\max(g)+1} = +\infty$. The expected revenue in the last situation, $\max(g) + 1$, is given by Formula (25):

$$R_{\max(g)+1} = \sum_{i|i\neq 0} \sum_{q\in K^i} c^i_q \bullet p^i_q \bullet \int_{h^d_{k,\max(g)}}^{h_{\max(g)+1}} f(x)dx \quad (25)$$

3.2. Objective Function

The objective function (26) is formulated to maximize the total expected revenue:

$$\max R(p^i_q) = \max \sum_{g=0}^{\max(g)+1} R_g \quad (26)$$

3.3. Constraints

The decision variable p^i_q must satisfy the following constraints:

(1) Price range constraint: p denotes the ceiling price.

$$0.5p \leq p^i_q \leq p \quad (27)$$

(2) Discrete price constraint: Due to operational requirements, the optimal price must be selected from the discrete price set Z.

$$\forall p^i_q \in Z \quad (28)$$

4. Solving Algorithm

Model (26) is a nonlinear programming problem (NLP) with a given domain of decision variable. Due to the diversity and complexity of the NLP problem, there is no universal exact solution algorithm, resulting in the fact that solving NLP problems is full of challenges in most cases. However, evolutionary algorithms, such as the Genetic Algorithm (GA) [39,40], Ant Colony Optimization algorithm (ACO) [41], Artificial Bee Colony algorithm (ABC) [42,43], and Particle Swarm Optimization algorithm (PSO) [44–51], are widely applied for solving NLP problems. Evolutionary algorithms have relatively simple structures and strong adaptability for majority optimization models, and particularly possess an advantage in balancing the accuracy and time complexity facing high-dimensional nonlinear optimization problems. Evolutionary algorithms essentially simulate the mechanism of natural evolution to perform a stochastic search in the solution space, iteratively generating the optimal solutions. PSO is among the evolutionary algorithms with the following distinct advantages:

(1) Its simple and easy implementation leads to the requirement of minimal programming expertise and coding effort;
(2) The small scale of the parameters simplifies parameter tuning;
(3) The fast convergence speed ensures that, since all particles in PSO share the global best position, they can quickly approach the best solution;

(4) There is a certain degree of global search capability by which the particles can escape local optima with a probability.

However, the basis enabling the PSO algorithm to search effectively in the given solution space at each iteration is the explicit identification of the best positions, namely, the personal historical best position and global best position, respectively. These two critical positions mark the areas in the solution space with a high probability of discovering the optimal solution, guiding all particles to move closer to them instead of making particles fluctuate completely randomly. The conventional PSO algorithm lacks adaptability and flexibility in updating these two positions, resulting in an insufficient accuracy and a slow convergence speed. In order to tackle this deficiency, scholars adopt the following strategies to optimize and record the best positions:

(1) Replace the personal historical best position with the weighted mean personal best position [45,47], or record the second-best position at each iteration [50];
(2) Maintain the variety in the particle swarm by preserving and expanding the size of the particles [46];
(3) Subdivide the entire particle swarm into several subpopulations with different functions under the condition of a big particle swarm [48];
(4) Introduce a new particle-position update mechanism combining particle confinement and dispersion to enhance the search space coverage in a large-sized particle swarm [49];
(5) Identify the particles with valuable directional information to guide the other particles to update their positions [51].

The above strategies enhance the probabilities of finding the new best positions through a certain mechanism, but each comes with its own limitations, especially expanding the size of the particle swarm to strengthen the search diversity, which, unexpectedly, brings additional time complexity. How to optimize the personal historical best position and global best position in certain steps of the iteration process to promote search efficiency and accuracy, while avoiding an expansion of the particle swarm size as much as possible, is the primary objective in designing the solution algorithm in this study. At last, a Sampling-Fitness-Strategy-based Particle Swarm Optimization (SFS-PSO) algorithm is proposed.

Some improved PSO algorithms integrate sampling strategies. For instance, Ref. [52] combines the GA with PSO to propose a hybrid evolutionary algorithm. It employs stratified sampling to enhance both global search and local search simultaneously. However, this algorithm is a serial combination of two evolutionary algorithms, resulting in a large sampling size. Ref. [53] also employs a two-stage sampling approach similar to this study. However, its sampling merely focuses on the particle positions and neglects the role of position-updating parameters. By contrast, indirectly generating new positions by sampling the position-updating parameters may potentially achieve a better performance in enhancing the search diversity of the algorithm. Ref. [54] focuses on how to enhance the local search ability of PSO to overcome the multi-modal optimization problems. Meanwhile there is insufficient attention paid to the roles of the personal historical best position and the global best position.

Therefore, in the proposed SFS-PSO, we optimize the personal historical best positions based on sampling the position-updating parameters to generate four specific positions, and the global best position by two-stage LHS sampling is performed. Thus, optimizing these two positions can improve both the local search diversity and global search efficiency without expanding the particle swarm size.

4.1. Conventional Particle Swarm Optimization with the Discrete Price Set Constraint

Construct a solution vector $\boldsymbol{p} = (p_1^1, p_2^1, \ldots p_g^d, \ldots, p_{\max(g)}^d)$ where each component p_g^d represents the train price with ranking g in the sold-out sequence. Set the maximum

number of particles P_{size} and the number of iterations $l = 1, 2, \ldots l_{\max}$. The initial position of the particle $H, H = 1, 2, \ldots P_{size}$ is recorded as $\boldsymbol{n}_H^{(0)}$.

$\mathrm{Ft}(\boldsymbol{n}_H^{(l)})$ is the fitness of $\boldsymbol{n}_H^{(l)}$. $Q_H^{(l)}$ and $Q^{(l)}$ denote the personal historical best position of particle H and global best position of the particle swarm at iteration l, respectively.

$$\boldsymbol{vs}_H^{(l)} = \boldsymbol{vs}_H^{(l-1)} + \phi_1 \bullet \boldsymbol{\varphi}_1 (Q^{(l)} - \boldsymbol{n}_H^{(l)}) + \phi_2 \bullet \boldsymbol{\varphi}_2 (Q_H^{(l)} - \boldsymbol{n}_H^{(l)}) \tag{29}$$

$$\hat{\boldsymbol{n}}_H^{(l+1)} = \boldsymbol{n}_H^{(l)} + \boldsymbol{vs}_H^{(l)} \tag{30}$$

$$\boldsymbol{n}_H^{(l+1)} = \Phi(\hat{\boldsymbol{n}}_H^{(l+1)}) \tag{31}$$

$$Q_H^{(l)} = \boldsymbol{n}_H^{(l)} | Ft(\boldsymbol{n}_H^{(l)}) \geq \forall Ft(\boldsymbol{n}_H^{(\hat{l})}), \forall \hat{l} \tag{32}$$

$$Q^{(l)} = \boldsymbol{n}_H^{(l)} | Ft(\boldsymbol{n}_H^{(l)}) \geq Ft(\boldsymbol{n}_H^{(\hat{l})}), \forall \hat{l}, \forall H \tag{33}$$

where $\boldsymbol{\varphi}_1$, $\boldsymbol{\varphi}_2$, and $\boldsymbol{\varphi}_3$ express random vectors with the same dimension as the solution vector $\boldsymbol{p} = (p_1^1, p_2^1, \ldots p_g^d, \ldots, p_{\max(g)}^d)$. $vs_H^{(l-1)}$ is the velocity which can be interpreted as inertia. ϕ_1 and ϕ_2 are just the weight parameters in the position-updating equation of the particles. Formulae (29)–(31) describe the particle update process. Formulae (32) and (33) record the personal historical best position and global best position. Equation (31) ensures that the prices satisfy the discrete constraint.

4.2. Sample Position-Updating Parameters to Optimize Personal Historical Best Position

Conventional PSO algorithms typically keep position-updating parameters unchanged throughout iterations. This inherent rigidity significantly limits their flexibility, adversely affecting both the convergence speed and solution accuracy. Therefore, a novel approach by dynamically sampling multiple position-updating parameters to yield several key positions is proposed. By comparing the fitness of the new key positions and existing personal historical best position, the personal historical best position for any given particle H is optimized iteratively which is illustrated in Figure 4.

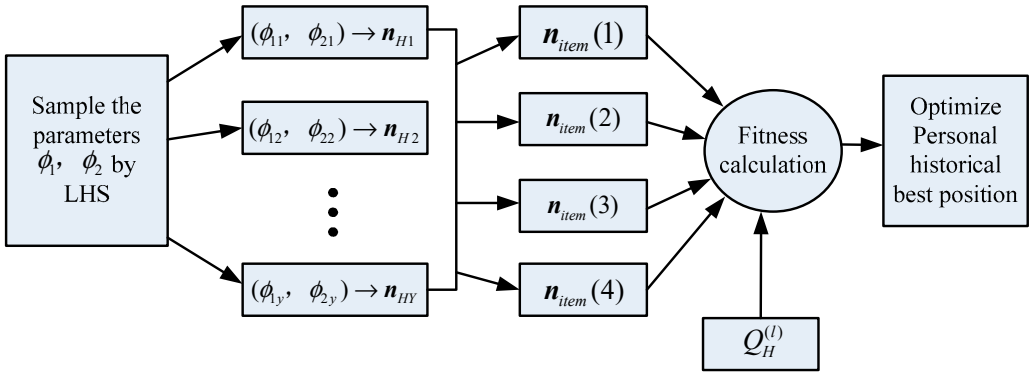

Figure 4. Optimization process of personal historical best position.

The process of updating the personal historical best position for particle H at any iteration l is as follows:

Step 1: Determine the sampling size Y and value range for ϕ_1 and ϕ_2.

Step 2: Use Latin Hypercube Sampling (LHS) to sample ϕ_1 and ϕ_2. Each set of samples of ϕ_1 and ϕ_2 generates a new position. A total of Y positions are obtained.

Step 3: For the generated Y positions, a position matrix of size $Y \bullet \max(g)$ can be constructed. Each row of this matrix represents a new position $\boldsymbol{n}_{Hy}$. The following four specific positions are extracted from the matrix:

Step 3.1: Specific position 1: $\boldsymbol{n}_{item}(1)$. Each dimension $\boldsymbol{n}_g(1)$ of $\boldsymbol{n}_{item}(1)$ is the mean value of the sampled set of positions in the same dimension.

$$\boldsymbol{n}_g(1) = \frac{\sum_{y=1}^{Y} \boldsymbol{n}(y,g)}{Y}, g = 1,2,\ldots \max(g), \forall H \tag{34}$$

Step 3.2: Specific position 2: $\boldsymbol{n}_{item}(2)$. Each dimension $\boldsymbol{n}_g(2)$ of this position is the median value of the sampled set of positions in the same dimension.

$$\boldsymbol{n}_g(2) = median(\boldsymbol{n}(y,g)), g = 1,2,\ldots \max(g), \forall H \tag{35}$$

Step 3.3: Specific position 3: $\boldsymbol{n}_{item}(3)$. Each dimension $\boldsymbol{n}_g(3)$ is set to the smaller value when comparing the maximum absolute value and the minimum absolute value of the sampled positions in the same dimension.

$$\boldsymbol{n}_g(3) = \begin{cases} \min(\boldsymbol{n}(:,g)), |\min(\boldsymbol{n}(:,g))| > |\max(\boldsymbol{n}(:,g))|, g = 1,2,\ldots \max(g), \forall H \\ \max(\boldsymbol{n}(:,g)), |\min(\boldsymbol{n}(:,g))| < |\max(\boldsymbol{n}(:,g))|, g = 1,2,\ldots \max(g), \forall H \end{cases} \tag{36}$$

Step 3.4: Specific position 4: $\boldsymbol{n}_{item}(4)$. Each dimension is set to the bigger value when comparing the maximum absolute value and the minimum absolute value of the sampled positions in the same dimension.

$$\boldsymbol{n}_g(4) = \begin{cases} \min(\boldsymbol{n}(:,g)), |\min(\boldsymbol{n}(:,g))| < |\max(\boldsymbol{n}(:,g))|, g = 1,2,\ldots \max(g), \forall H \\ \max(\boldsymbol{n}(:,g)), |\min(\boldsymbol{n}(:,g))| > |\max(\boldsymbol{n}(:,g))|, g = 1,2,\ldots \max(g), \forall H \end{cases} \tag{37}$$

Step 4: The fitness of the specific positions 1~4 and the current personal historical best position $Q_H^{(l)}$ are calculated. The one with highest fitness among these five positions is selected as the replacement for the new personal historical best position.

4.3. Sampling-Based Local Search to Optimize Global Best Position

To further promote the accuracy, it is necessary to optimize the current global best position by leveraging all global best positions recorded during the iterative process.

For any dimension g of the global best position $Q^{(l)}$ at iteration l, initialize $\boldsymbol{n}_g^{(l)}(1) = \boldsymbol{n}_g^{(l)}(2) = Q_g^{(l)}$. The minimum element of the global best position is designated as $\min(Q_g^{(l)}), \forall g$. Finally, the weighted average value for each dimension of the global best position $avg(Q_g^{(l)})$ weighted by the fitness of all historical global best positions is obtained by Formula (38):

$$avg(Q_g^{(l)}) = \sum_{l=1} \frac{Ft(Q^{(l)})}{\sum_{l=1} Ft(Q^{(l)})} \bullet \frac{\min(Q_g^{(l)}) + \max(Q_g^{(l)})}{2}, \forall g \tag{38}$$

$avg(Q_g^{(l)})$ corresponds to the central point of the key region constituted by the historical global best positions in the solution space. The proximity to $avg(Q_g^{(l)})$ implies a higher probability of seeking out a new global best position in the search. Update $\boldsymbol{n}_g^{(l)}(1)$ and $\boldsymbol{n}_g^{(l)}(2)$:

$$\boldsymbol{n}_g^{(l)}(1) = \min(Q_g^{(l)}) + \text{rand}() \bullet (avg(Q_g^{(l)}) - \min(Q_g^{(l)}) \tag{39}$$

$$\boldsymbol{n}_g^{(l)}(2) = avg(Q_g^{(l)}) + \text{rand}() \bullet (\max(Q_g^{(l)}) - avg(Q_g^{(l)}) \tag{40}$$

where $rand()$ stands for a random number between 0 and 1. Next, LHS-based dual sampling is adopted for the local search in key regions. It involves two sampling phases: a coarse sampling within a broader range to point to a roughly best position, followed by a fine sampling within a narrowed range to find a more precise global best position. The first sampling interval is determined by the following formula:

$$\begin{cases} b_{f\min} = \max\{Q_g^{(l)} \bullet (1 - sign(Q_g^{(l)}) \bullet \frac{l_{\max} - l}{l_{\max}}), \min[\boldsymbol{n}_g^{(l)}(1), \boldsymbol{n}_g^{(l)}(2)]\} \\ b_{f\max} = \min\{Q_g^{(l)} \bullet (1 + sign(Q_g^{(l)}) \bullet \frac{l_{\max} - l}{l_{\max}}), \max[\boldsymbol{n}_g^{(l)}(1), \boldsymbol{n}_g^{(l)}(2)]\} \end{cases} \tag{41}$$

where $b_{f\min}$ and $b_{f\max}$ compose a sampling interval $[b_{f\min}, b_{f\max}]$ where the first sampling is performed, and the sampling size $\hat{Y}^{(l)}$ is determined by Equation (42).

$$\hat{Y}^{(l)} = A \bullet \frac{l_{\max} - l}{l_{\max}} \tag{42}$$

Thus, a sample matrix with a size of $\hat{Y}^{(l)} \times \max(g)$ where each row represents a new position, is constructed. Generally, we set $A = 10$ to control the sampling scale. By calculating the fitness of each new position and $Q^{(l)}$, the position exhibiting the highest fitness is recognized and designated as $\boldsymbol{n}^{(l)}(3)$. Subsequently, we perform the second sample from the sampling interval $[b_{s\min}, b_{s\max}]$.

$$\begin{cases} b_{s\min} = \max\{\boldsymbol{n}_g^{(l)}(3) \bullet [1 - sign(\boldsymbol{n}_g^{(l)}(3)) \bullet rand() \bullet \frac{l_{\max} - l}{l_{\max}}], b_{f\min}\} \\ b_{s\max} = \min\{\boldsymbol{n}_g^{(l)}(3) \bullet [1 + sign(\boldsymbol{n}_g^{(l)}(3)) \bullet rand() \bullet \frac{l_{\max} - l}{l_{\max}}], b_{f\max}\} \end{cases} \tag{43}$$

Due to $b_{f\min} \leq b_{s\min}$ and $b_{f\max} \geq b_{s\max}$, the second sampling interval is smaller than the first sampling interval which converts the first coarse local search to the second fine local search. Moreover, as the iteration progresses, the sampling interval progressively narrows, thereby intensifying the local search. Similarly, a position matrix with a size of $\hat{Y}^{(l)} \times \max(g)$ is produced after the second sampling. Select the position with the highest fitness as the new global best position.

4.4. The Process of SFS-PSO

Based on the above analysis, the process of the SFS-PSO in this paper is as follows:

Step 1: Initialize all parameters. Set the maximum number of iterations $l_{\max}$ and the particle swarm size P_{size}.

Step 2: Generate one particle $\boldsymbol{n}_H^{(0)}$ to form an initial particle swarm. At this time, $H = 1$, $\boldsymbol{vs}_H^{(0)} = 0$, and $n_H^{(0)} = Q_H^{(0)} = Q^{(0)}$. Set $l = 1$, and then begin the iteration.

Step 3: Sample position-updating parameters to optimize personal historical best position for each particle.

Step 3.1: Determine the sampling size and interval. Generate multiple samples of parameters ϕ_1 and ϕ_2 through LHS.

Step 3.2: With sets of samples of ϕ_1 and ϕ_2, a total of Y positions which compose a position matrix of size $Y \bullet \max(g)$ is obtained.

Step 3.3: Use Equations (34)–(37) to produce four specific intermediate positions $\boldsymbol{n}_{item}(1)$, $\boldsymbol{n}_{item}(2)$, $\boldsymbol{n}_{item}(3)$, and $\boldsymbol{n}_{item}(4)$ from the position matrix.

Step 3.4: Input the four specific intermediate positions and the current personal historical best position $Q_H^{(l)}$ into the objective Function (26) to calculate the fitness. The personal historical best position is optimized based on whether the fitness can be improved.

Step 4: Perform a sample-based local search to optimize the global best position.

Step 4.1: For any dimension g, initialize $\boldsymbol{n}_g^{(l)}(1) = \boldsymbol{n}_g^{(l)}(2) = Q_g^{(l)}$. Calculate the weighted average value of the global best position $avg(Q_g^{(l)})$ by Formula (38). Then, update $\boldsymbol{n}_g^{(l)}(1)$ and $\boldsymbol{n}_g^{(l)}(2)$ using Formulae (39) and (40).

Step 4.2: Define an initial sampling interval in the vicinity of the global best position $Q^{(l)}$ using Formula (41). Perform LHS $\hat{Y}^{(l)}$ times based on the sampling interval $[b_{f\min}, b_{f\max}]$.

Step 4.3: Record the new global best position as $\boldsymbol{n}^{(l)}(3)$ according to the fitness of the $\hat{Y}^{(l)}$ new positions and $Q^{(l)}$.

Step 4.4: Define a smaller sampling interval with $\boldsymbol{n}^{(l)}(3)$ at its center for the second fine search by Equation (43). Adopt LHS again to generate $\hat{Y}^{(l)}$ new positions.

Step 4.5: Optimize the global best position according to the highest fitness.

Step 5: On the basis of completing the optimization of the personal historical best position and global best position, update all particle positions through Equations (29)–(31).

Step 6: Update the personal historical best positions and global best position by Equations (32)–(33).

Step 7: If figuring out the new global best position (optimal solution), the SFS-PSO algorithm has demonstrated expected effectiveness. In this case, the particle swarm should be expanded to directly intensify the SFS-PSO. Then, go to **Step 8;** otherwise, turn to **Step 9.**

Step 8: If $H = P_{size}$, then go to **Step 9**; otherwise, increase particles, let $H = H + 1$, and turn back to **Step 3.**

Step 9: If $l < l_{\max}$, then set $l = l + 1$ and reset $H = 1$, and go back to **Step 3;** otherwise, proceed to **Step 10.**

Step 10: End the iteration. Output the global best position to derive the optimal price scheme.

The SFS-PSO algorithm is given below (Algorithm 1).

4.5. The Time Complexity of SFS-PSO

Although both particle-position updates and sampling consume time, the time cost of the solving algorithm is primarily dominated by fitness calculations. Since the number of fitness evaluations per iteration in SFS-PSO is not fixed, the number of fitness evaluations is used as the metric to ensure a fair comparison with the conventional PSO. Thus, the time complexity can be represented by only taking account into the cost of fitness evaluations (the number of fitness evaluations).

The conventional PSO possesses the time complexity of $O(P_{size} \bullet l_{\max})$, while the time complexity of the proposed SFS-PSO is as follows:

$$O(\sum_{l=1}^{l_{\max}} \sum_{H^{(l)}=1}^{\max(H^{(l)})} H^{(l)} \bullet 4) + O(\sum_{l=1}^{l_{\max}} \max(H^{(l)}) \bullet 2 \bullet Y^{(l)}) + O(\sum_{l=1}^{l_{\max}} \sum_{H^{(l)}=1}^{\max(H^{(l)})} H^{(l)}) \quad (44)$$

where $Y^{(l)}$ is determined by the sample size A. Due to the fact that the number of particles $\max(H^{(l)})$ at each iteration is not fixed, the time complexity of SFS-PSO is mainly related to the sample size A.

Algorithm 1: SFS-PSO

Input: currently implemented price scheme, passenger flow volume
Output: the optimal price scheme, the maximum expected revenue
Begin
Initialization, $l_{\max}, P_{size}, \boldsymbol{n}_H^{(0)}$
$Q_H^{(0)} \leftarrow \boldsymbol{n}_H^{(0)}$
$Q^{(0)} \leftarrow \boldsymbol{n}_H^{(0)}$
For $l \leftarrow 1$. to $l_{\max}$ do:
For $H \leftarrow 1$. to P_{size} do:
For $y \leftarrow 1$ to Y do for each particle H:
$\phi_1, \phi_2 \leftarrow sampling$
$\boldsymbol{n}_{item}(1), \boldsymbol{n}_{item}(2), \boldsymbol{n}_{item}(3), \boldsymbol{n}_{item}(4) \leftarrow Eqs(34) \sim (37)$
$Q_H^{(l)} \leftarrow position \left| \max Fitness(\boldsymbol{n}_{item}(1), \boldsymbol{n}_{item}(2), \boldsymbol{n}_{item}(3), \boldsymbol{n}_{item}(4)) \right.$
For $g \leftarrow 1$ to $\max(g)$ do:
$avg(Q_g^{(l)})_1, \boldsymbol{n}_g^{(l)}(1), \boldsymbol{n}_g^{(l)}(2) \leftarrow Eqs(38) \sim (44)$
For $y \leftarrow 1$ to $\hat{Y}^{(l)}$ do:
Obtain a new position by sampling from $[b_{f\min}, b_{f\max}]$
$\boldsymbol{n}^{(l)}(3) \leftarrow$ the position with the maximum fitness
For $y \leftarrow 1$ to $\hat{Y}^{(l)}$ do:
Obtain a new position by sampling from $[b_{s\min}, b_{s\max}]$
$Q^{(l)}(3) \leftarrow$ the position with the maximum fitness
$H \leftarrow Eqs(29) \sim (31)$
$Q^{(l)}, Q_H^{(l)} \leftarrow Eqs(32) \sim (33)$
If figuring out a new global best position:
Continue
Else:
$H \leftarrow 1$
$\boldsymbol{n}_H^{(l)} \leftarrow Q^{(l)}$
Return $\boldsymbol{n}_H^{(l)}, Q^{(l)}, Q_H^{(l)}$
Return $Q^{(l)}$ and the maximum fitness
End

5. Case Analysis

5.1. Data Acquisition

Take the OD pair from Beijing-South station to Shanghai-Hongqiao station as a case study. Referring to the train classification criteria from the literature [55], nine representative trains providing travel service between the OD pair are divided into four categories ($d = 0, 1, 2, 3$) based on the travel time, namely, high-class trains ($d = 1$) with a travel time of approximately 4.5 h, standard trains ($d = 2$) with a travel time of about 5.5 h, and low-class trains ($d = 3$), whose travel time exceeds 6 h. In addition, all trains constitute the largest train category ($d = 0$). Each train category comprises three trains with a similar departure time, as shown in Table 2. The currently implemented discrete price set includes seven levels of prices which are listed in Table 3.

Table 2. Train details.

Train	Departure Time	Travel Time (Unit: min)	Current Price (Unit: CNY)	Category	Number of Tickets Allocated
G19	16:00	268	662	High-class	747
G15	14:00	272	662	High-class	880
G17	15:00	274	662	High-class	778
G115	09:10	336	626	Standard	39
G121	10:05	337	626	Standard	102
G117	09:20	340	598	Standard	122
G151	15:49	372	553	Low-class	36
G147	14:27	373	576	Low-class	61
G141	13:34	394	612	Low-class	23

Table 3. Currently active discrete price set.

Level	Price (Unit: CNY)
1	662
2	626
3	612
4	598
5	576
6	553
7	526

5.2. Passenger Classification and Parameter Estimation

The period from 1 July 2024 to 31 August 2024 is selected as the reference date to calculate the passenger flow with a mean value of $\mu = 2708$ and standard deviation of $\sigma = 459.6$. Referring to the economic-value-based passenger classification in the literature [13,19], all passengers are categorized into business passengers ($j = 1$) and ordinary passengers ($j = 2$) based on the median cost of the trip for all passengers. Each passenger category constitutes 50% of the total passengers. Table 4 shows that the proportions of loyal passengers to various train categories in each passenger group are obtained separately through Formula (2). Among business passengers, 14% are loyal to low-class trains, 36% exhibit loyalty to high-class trains, and 11% are loyal passengers of standard trains. Consequently, loyal passengers account for 61% among business passengers, while they account for 51% among ordinary passengers. High-class trains provide the highest quality of service, leading to a greater share of loyal passengers [25].

Table 4. The proportions of loyal passengers in passenger groups.

Passenger Category	The Proportion in Total Passengers (%)	Train Category	The Proportion of Loyal Passengers in This Passenger Category for Corresponding Train Category (%)
Business passengers	50%	Low-class	14%
		High-class	36%
		Standard	11%
Ordinary passengers	50%	Low-class	23%
		High-class	12%
		Standard	16%

The benchmark of the time value is set as $v_{0,j} = 0, j = 1, 2$. The time value of business passengers is naturally higher than that of ordinary passengers. With reference to the five quintiles of income defined by China's National Bureau of Statistics, different income

groups exhibit distinct time values. Due to the fact that passengers on the Beijing–Shanghai corridor are usually considered to possess relatively higher incomes, we adopt the median incomes of the highest and second-highest income groups in five income groups to estimate their time value. The parameters $\omega_j, j = 1, 2$ of the time values for business passengers and ordinary passengers are estimated, respectively, under the condition that the median incomes cover 80% of passengers in their respective income groups. The floor of the generalized cost expectations $f_{0,\,1}$ and $f_{0,\,2}$ are set at the highest-level price of 662 and the median-level price of 598 from the discrete price set. Similarly, the parameters $\overline{\omega}_j, j = 1, 2$ in the exponential probability functions of the generalized cost expectation is subsequently evaluated and presented in Table 5.

Table 5. Parameter estimation.

	Business Passenger j = 1	**Ordinary Passenger j = 2**
The minimum time value $v_{0,j}$	0	0
Median annual income per capita (unit: CNY)	98,809	53,395
Time value per minute (unit: CNY/min)	0.7797	0.4214
The parameters ω_j of the exponential probability functions for time value	2.064	3.82
Lower limit of generalized cost expectations $f_{0,j}$ (unit: CNY)	662	598
The parameters $\overline{\omega}_j$ of the exponential probability functions for price expectations	0.00886	0.0154

5.3. Result Analysis

The parameter configuration for PSO lacks universal rules and often requires customization based on application scenarios and empirical knowledge. Comprehensively considering the time cost and solution accuracy, we set the maximum number of iterations $l_{\max} = 100$, the sampling size $Y = 10$, $A = 10$, and the maximum particle swarm size $P_{size} = 10$. The initial solution of each train is set as the median price of CNY 598. Using Python 3.7 as the software to run the proposed SFS-PSO, due to the randomness of the iterative process, ten random runs are conducted. The corresponding expected revenue is presented in Table 6. The maximum expected revenue observed (in the fourth run) among these ten runs is designated as Case 1. The actual revenue 1,479,120 of the currently implemented price scheme is selected as a comparison, in Case 2.

Table 6. The expected revenues of 10 random runs.

Run	**1**	**2**	**3**	**4**	**5**
Expected revenue **(CNY)**	1,492,345	1,478,830	1,486,688	1,504,230	1,503,232
Comparing Case 2 +%	0.89%	−0.02%	0.51%	1.7%	1.63%
Run	6	7	8	9	10
Expected revenue **(CNY)**	1,467,893	1,479,204	1,486,050	1,475,466	1,495,352
Comparing Case 2 +%	−0.76%	0.01%	0.47%	−0.25%	1.1%

Figure 5 illustrates the iterative process of Case 1 where the SFS-PSO algorithm converged to the maximum expected revenue of 1,504,230 CNY. Table 6 demonstrates that, in the majority of runs (7 out of 10), each maximum expected revenue obtained through SFS-PSO solving the optimization model achieves the objective of revenue improvement. However, due to the inherent randomness of evolutionary algorithms and the practical constraint of maximum iterations, the optimized expected revenue may fall short of the actual

revenue of Case 2 in a minority of runs. The fourth run achieved the maximum expected revenue, realizing a 1.7% growth compared to the expected revenue of 1,479,120 CNY in Case 2. Assuming the expected revenue fits the normal distribution and based on the maximum expected revenue samples from 10 random runs in Table 6, the results show that the mean and standard deviation are 1,486,929 and 11,336, respectively; thus, the 95% confidence interval for the expected revenue is between CNY 1,484,706 and CNY 148,915.

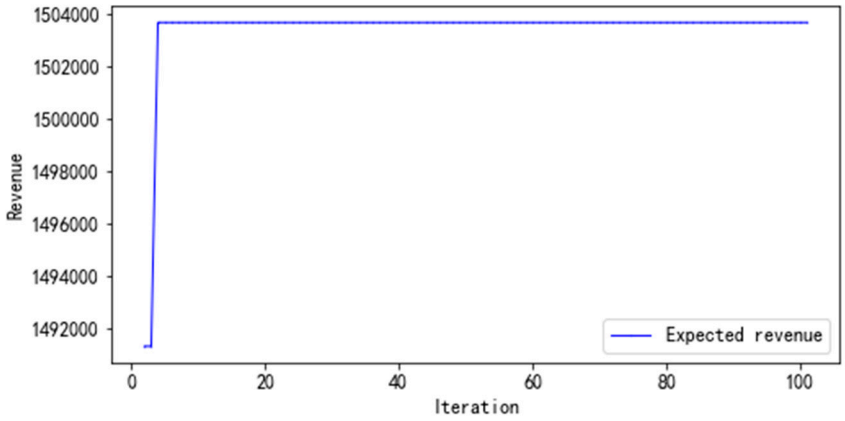

Figure 5. Iterative Process of Case 1.

Tables 7 and 8 detail the optimal price scheme. Trains G115 and G121 are assigned the highest price of 626 CNY, while trains G117, G141, and G147 possess the lowest price of 598 CNY. From the view of the train category, standard trains achieve the highest average price, followed by high-class trains, and low-class trains with the lowest average price.

Table 9 lists the train choice probabilities of non-loyal passengers in each passenger category under the optimal price scheme. Non-loyal passengers exclusively selecting G117 and G19 indicates that standard trains lack distinct advantages in either price or travel time. Once G117 and G19 are sold out, non-loyal passengers opt to forgo high-speed railway. Table 10 presents the sequence of sold-out trains and the corresponding passenger flow. Key observations include the following: (1) Within the same train category, the sell-out sequence aligns with the price ranking. (2) The optimal price scheme allows loyal passengers to be able to purchase tickets for their preferred trains in all train categories, guaranteeing the widest choice for them. (3) In view of the highest proportion of business passengers showing loyalty to high-class trains, the optimal price scheme guarantees the high-class trains manage to sell out last, effectively satisfying the travel demands of loyal passengers in the business passengers category.

Table 7. The optimal price scheme of Case 1.

Train	The Initial Price	Discrete Price Level	The Optimal Price (Unit: CNY)	Train Category
G115	612	2	626	High-class
G121	626	2	626	Standard
G15	662	3	612	High-class
G151	598	3	612	Low-class
G17	662	3	612	High-class
G19	662	3	612	Standard
G117	576	4	598	Standard
G141	576	4	598	Low-class
G147	553	4	598	Low-class

Table 8. The average prices of each train category in Case 1.

Train Category	The Average Price (Unit: CNY)
High-class	612
Standard	616
Low-class	602

Table 9. Choice probabilities of non-loyal passengers in each passenger category in Case 1.

Train	Passenger Category	The Choice Probability of Non-Loyal Passengers in This Passenger Category
G117	Business Passengers	33.1%
	Ordinary Passengers	52.4%
G19	Business Passengers	66.9%
	Ordinary Passengers	47.6%

Table 10. The sell-out sequence and corresponding passenger flow of trains in Case 1.

Train	The Corresponding Passenger Flow	Train Category	Whether Loyal Passengers Have Purchased the Tickets for the Train	The Sell-Out Sequence in This Train Category	The Sell-Out Sequence in All Trains
G117	257	Standard	Yes	1	1
G147	306	Low-class	Yes	1	2
G141	422	Low-class	Yes	2	3
G115	451	Standard	Yes	2	4
G151	603	Low-class	Yes	3	5
G121	963	Standard	Yes	2	6
G19	1196	High-class	Yes	1	7
G15	4130	High-class	Yes	2	8
G17	6724	High-class	Yes	3	9

5.4. Sensitivity Analysis

The diverse preferences and differentiated choice processes of passengers fundamentally derive from their heterogeneity that can be intuitively observed through two aspects: the proportions of each passenger category in total passengers and the proportions of loyal passengers in each passenger category. These two indicators play critical roles in optimizing the price scheme to improve the expected revenue. In the following section, a sensitivity analysis on these two indicators, respectively, is implemented.

5.4.1. Impact of Different Proportions of Passenger Categories in Total Passengers

During the off-peak period, the business passenger group is shrinking markedly [36]. Assume the proportion of business passengers drops from 50% to 20%, while the proportion of ordinary passengers increases from 50% to 80% (Table 11). All other assumptions, parameter values, and the proportions of loyal passengers to each train category remain unchanged. The above situation constitutes Case 3.

The maximum expected revenue in Case 3 is obtained using the SFS-PSO proposed in Section 4, with the maximum iteration number of 50. The iteration process is shown in Figure 6. A comparison of the total expected revenue between Case 3 and Case 1 is presented in Table 12 where the proportion of business passengers decreases from 50% to 20% and the total expected revenue drops from 1,504,230 CNY to 1,370,435 CNY with a reduction of 8.9%.

Table 11. The comparison of proportions of different passenger categories between Case 1 and Case 3.

Passenger Category	The Proportion of This Passenger Category in Total Passengers (%)		Train Category	The Proportion of Loyal Passengers in This Passenger Category to Corresponding Train Category (%)
	Case 1	Case 3		
Business passengers	50%	20%	Low-class High-class Standard	14% 36% 11%
Ordinary passengers	50%	80%	Low-class High-class Standard	23% 12% 16%

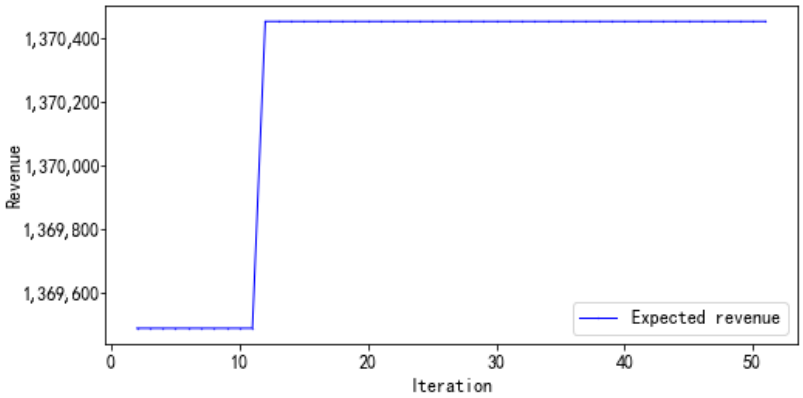

Figure 6. Iterative process in Case 3.

Table 12. Impact of different proportions of passenger categories on expected revenue.

	Total Expected Revenue	±%
Case 1	1,504,230	/
Case 3	1,370,435	−8.9%

Table 11 shows that the loyal passengers account for a proportion of 61% in business passengers. In contrast, loyal passengers make up 51% of ordinary passengers, a significant ten percent lower than that of business passengers. Moreover, loyal passengers opt out of high-speed railway trips only when all tickets of their preferred train category are sold out, bringing a possible higher revenue. Therefore, the reduced proportion of business passengers (an increase in the share of ordinary passengers) inevitably leads to a decline (Table 12) in total expected revenue under stable passenger preferences.

Table 13 details the comparison of the average optimal prices between Case 1 and Case 3. The dropped proportion of business passengers causes an overall reduction in optimal prices for high-class trains and standard trains which possess relatively higher proportions of loyal passengers among business passengers.

Table 13. Comparison of optimal average prices of each train category.

Train Category	Average Price (Unit: CNY)	
	Case 1	Case 3
High-class	612	604
Standard	616	600
Low-class	602	612

5.4.2. Impact of Different Proportions of Loyal Passengers in Passenger Categories

Still maintaining all assumptions and parameter values unchanged, we conduct the simulation cases by adjusting the proportion of loyal passengers in 5% increments every time. Thus, Cases 4, 5, 6, and 7 are constructed as shown in Table 14. Case 4 and Case 5 represent a decrease in the proportions of loyal passengers. Case 6 and Case 7 increase the proportions of loyal passengers.

Table 14. The proportions of loyal passengers in Cases 4~7.

Passenger Category	The Proportion of This Passenger Category in Total Passengers (%)	Train Category	The Proportion of Loyal Passengers in this Passenger Category (%) Comparing to Case 1			
			Case 4 (−5%)	Case 5 (−10%)	Case 6 (+5%)	Case 7 (+10%)
Business passengers	50%	Low-class	9%	4%	19%	24%
		High-class	31%	26%	41%	46%
		Standard	6%	1%	16%	21%
Ordinary passengers	50%	Low-class	17%	13%	28%	33%
		High-class	7%	2%	17%	22%
		Standard	11%	6%	21%	26%

Figure 7 illustrates the iterative process of solving Cases 4~7 using the proposed SFS-PSO, ultimately comparing the total expected revenue in Table 15. The results demonstrate that Case 4 and Case 5 reduce the proportions of loyal passengers in all passengers to 41% and 26% from 56% in Case 1, causing a decline in the total expected revenue from 1,504,230 CNY to 1,408,166 CNY (−6.38%) and 1,239,320 CNY (−17.62%), respectively. Conversely, the increase in the proportions of loyal passengers from 56% in Case 1 to 71% (Case 6) and 86% (Case 7) raises the corresponding expected revenue from 1,504,230 CNY to 1,534,030 CNY (+1.99%) and 1,568,289 CNY (+4.26%). Figure 8 describes an approximate consistent fluctuation trend of the two curves representing the proportions of loyal passengers and the total expected revenue, respectively. The trend confirms the roughly positive correlation between them and further validates the importance of loyal passengers in improving the market revenue for high-speed railways.

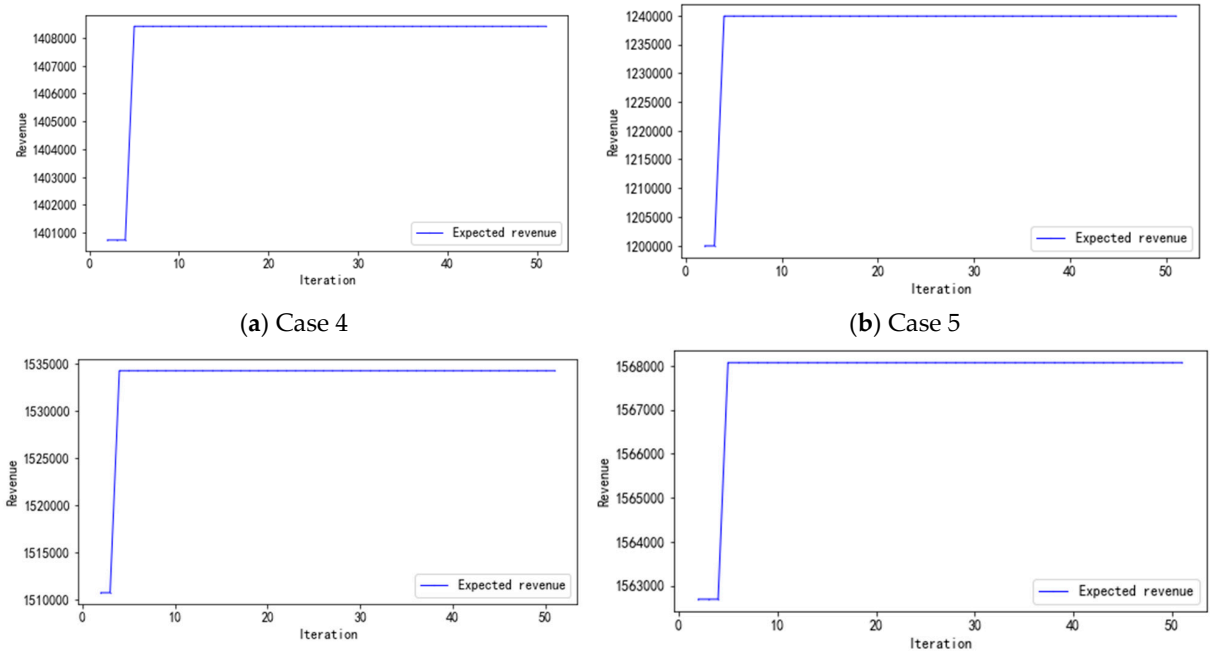

(**a**) Case 4 (**b**) Case 5

(**c**) Case 6 (**d**) Case 7

Figure 7. Iterative processes in Cases 4~7.

Table 15. The influence of different proportions of loyal passengers on expected revenue.

Case	Total Expected Revenue (Unit: CNY)	+% (Compared to Case 1)	Proportion of Loyal Passengers in Total Passengers
Case 1	1,504,230	/	56%
Case 4	1,408,166	−6.38%	41%
Case 5	1,239,320	−17.62%	26%
Case 6	1,534,030	1.99%	71%
Case 7	1,568,289	4.26%	86%

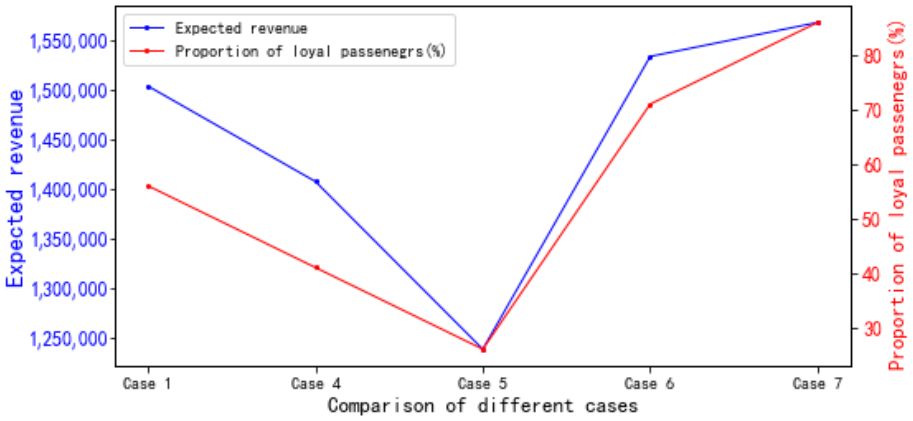

Figure 8. Relationship between the proportions of loyal passengers and total expected revenue.

5.5. The Performance of SFS-PSO

Since this paper focuses on exploring hybrid passenger choice behaviors to construct the pricing optimization model, the proposed SFS-PSO works primarily as a solution approach and is not being investigated in an in-depth algorithmic performance experiment [56]. Therefore, the only comparison with the conventional PSO to briefly demonstrate the performance of the SFS-PSO is implemented.

5.5.1. Experiments on the Expected Revenue Function

Input the identical initial solution to both the SFS-PSO and conventional PSO to solve the pricing optimization model (26). Each solving algorithm is implemented 10 times. Table 16 compares the results. The proposed SFS-PSO achieved an average total expected revenue of 1,486,929 and maximum total expected revenue of 1,504,230, respectively, surpassing the conventional PSO by 1.84% and 0.9%, thereby validating the effectiveness and advancement of the SFS-PSO in terms of solution accuracy.

Table 16. Accuracy comparison on expected revenue function.

	SFS-PSO	Conventional PSO	±%
Average total expected revenue (CNY)	1,486,929	1,460,077	1.84%
Maximum total expected revenue (CNY)	1,504,230	1,490,820	0.9%

Based on the analysis in Section 5.5, the time complexity of the conventional PSO algorithm is primarily influenced by the swarm size P_{size}, while that of SFS-PSO is mainly determined by the sampling size (Y, A). The following scaling experiments investigate these two factors separately:

(1) Scaling experiment on varying particle counts. Maintain the maximum number of iterations $l_{\max} = 100$, and the sampling size $Y = 10$, $A = 10$. Make the particle swarm size

P_{size} vary from 5 to 30 with an interval of 5 (5, 10, 15, 20, 25, and 30). Due to the expensive computational time of fitness in the cases, each algorithm is executed twice under each given swarm size. The average time consumption is recorded in Figure 9 where the vertical axis represents the wall-clock runtime, while the horizontal axis represents different particle swarm sizes. It can be seen that the SFS-PSO holds a marked advantage in wall-clock time when the number of particles surpasses 25.

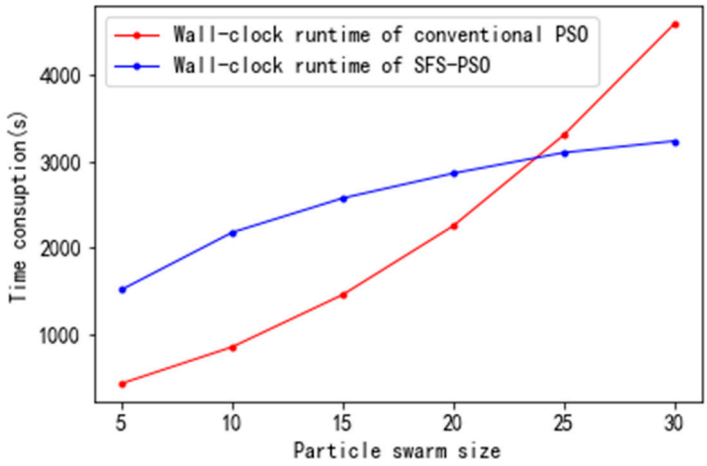

Figure 9. Comparison of wall-clock runtime between the SFS-PSO and conventional PSO under different particle swarm size.

(2) Scaling experiment on the sampling size. Maintain the maximum number of iterations $l_{\max} = 100$, and the particle size $P_{size} = 10$. The sampling size (Y, A) was set to (5, 5), (10, 10), (20, 20), and (30, 30). The SFS-PSO is executed twice under each given sampling size. The comparison result is illustrated in Figure 10 where the vertical axis represents the wall-clock runtime, while the horizontal axis expresses different sampling sizes. A clear positive correlation can be observed between the expanding sampling size (Y, A) and the increasing time complexity of the SFS-PSO.

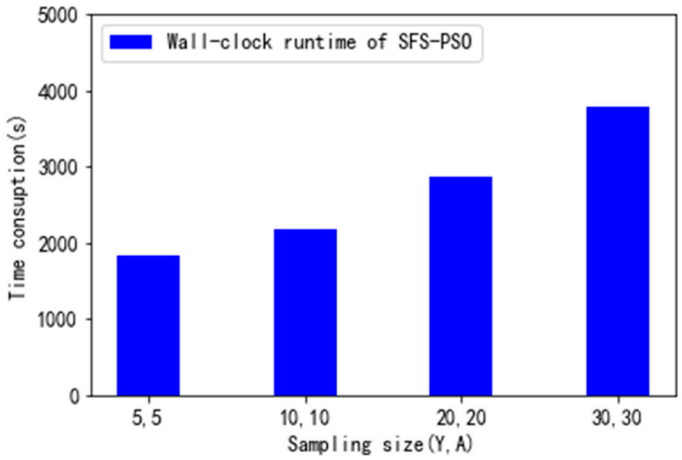

Figure 10. Comparison of wall-clock runtime under different sampling sizes for SFS-PSO.

5.5.2. Experiments on Standard Benchmark Functions

As described in Section 4.5, the number of fitness evaluations per iteration in the SFS-PSO is not fixed. To ensure a fair testing and comparison, the number of fitness evaluations is selected as a representation of time complexity. The SFS-PSO is compared with the conventional PSO from two perspectives: the solution accuracy under the same maximum fitness evaluations, and the number of fitness evaluations required to meet the

same accuracy requirement. Furthermore, the sampling strategy is the featured design of the SFS-PSO; thus, the impact of the sampling size on its performance is tested.

(1) The search accuracy under the same maximum fitness evaluations. Functions Sphere and Rosenbrock are selected as the standard benchmark to test and compare the performance of the SFS-PSO and the conventional PSO. The parameter settings are listed in Table 17. The maximum fitness evaluation is given as 30,000. Each algorithm is implemented 10 times. The result is shown in Table 18, which indicates that, under the maximum fitness evaluations of 30,000, SFS-PSO demonstrates a significantly higher precision than the conventional PSO algorithm in both the Sphere and Rosenbrock functions, improving the performance of the conventional PSO by at least two orders of magnitude and validating its effectiveness. Although the average computation time of SFS-PSO is bigger than that of the conventional PSO, the time consumption remains within an acceptable range.

Table 17. Parameter settings.

	Dimension	Particle Swarm Size P_{size}	The Maximum Iteration Count $l_{\max}$	The Maximum Fitness Evaluation I	Sampling Interval for ϕ_1	Sampling Interval for ϕ_2	Sampling Size (Y,A)
Conventional PSO	30	20	1500	30,000	/	/	/
SFS-PSO	30	20	/	30,000	[1.25, 2.75]	[0.5, 2.25]	(10, 10)

Table 18. Comparison results under the same maximum fitness evaluation $I = 30000$.

Test Function	Algorithm	The Optimal Value of Test Function	Average Value of Test Function	Average Time Consumption (Unit: sec)
Sphere	**Conventional PSO**	49.134	3.407×10^3	1.78
	SFS-PSO	1.873×10^{-32}	1.651×10^{-30}	2.52
Rosenbrock	**Conventional PSO**	23.821	6.118×10^3	1.89
	SFS-PSO	0.901	1.034×10^2	3.13

(2) The search efficiency under the same accuracy requirement. The parameters in Table 17 remain unchanged. Using the Rosenbrock function as the benchmark with a precision threshold $\varepsilon \leq 200$ (the value of the Rosenbrock function falls below 200), and the maximum fitness evaluation still set as $I = 30000$, each algorithm is tested 30 times. For each run, the following are recorded: (1) whether the algorithm met the precision requirement under the maximum fitness evaluation limit, and (2) the numbers of fitness evaluations required to reach the precision threshold. The result is shown in Table 19. It indicates that SFS-PSO significantly outperformed the conventional PSO in both the number of successful runs (those meeting the precision requirement) out of 30 tests and the average number of iterations as well as the optimal number of iterations required across all successful runs. The comparison in Table 19 verifies the search efficiency of SFS-PSO.

Table 19. The number of fitness evaluations required to meet the same accuracy requirement.

Test Function	Algorithm	The Number of Runs Meeting the Precision Threshold	The Total Number of Runs	The Optimal Number of Fitness Evaluations Required	The Average Number of Fitness Evaluations Required
Rosenbrock	**Conventional PSO**	5	30	1980	8560
	SFS-PSO	26	30	438	3762

(3) The influence of the sampling size on the performance of SFS-PSO. Based on the qualitative assessment from Equation (44), the time complexity of SFS-PSO is related to the

sampling size A. Therefore, the impact of different sampling sizes on SFS-PSO's performance under the same maximum fitness evaluation $I = 30000$ is tested with Rosenbrock for 10 times. The other parameters in Table 17 remain unchanged. The corresponding results are presented in Table 20. Table 20 suggests that, under the same maximum fitness evaluation, increasing the sampling size at each iteration does not lead to substantial improvements in terms of the optimal function value as well as the average function value. Therefore, considering that expanding the sampling size will prolong the duration of each iteration, maintaining a moderate sampling size is sufficient.

Table 20. The influence of sampling sizes (Y, A) under the same maximum fitness evaluation $I = 30000$.

Test Function	Sampling Size	The Optimal Value of Test Function	Average Value of Test Function
Rosenbrock	(10, 10)	0.901	1.034×10^2
	(20, 20)	0.737	1.631×10^2
	(50, 50)	0.801	0.802×10^2
	(100, 100)	0.577	1.173×10^2

6. Conclusions and Suggestions

6.1. Conclusions

The key conclusions from the case analysis are as follows:

(1) The expected revenue is increased by 1.7% (Table 8) through the proposed pricing approach. Although the revenue improvement appears marginal, an increase of 1.7% will generate additional revenue amounting to nearly tens of billions of CNY if the pricing model is applied to the entire high-speed railway network across China.

(2) The optimal pricing scheme ensures loyal passengers are able to purchase tickets of all train categories (Table 10), thereby maximizing the fulfillment of travel demands for loyal passengers. This point has benefits for high-speed railway marketing to achieve long-term returns.

(3) Due to the fact that the proportion of loyal passengers among business passengers is relatively higher than that among ordinary passengers (Table 4), a reduction in the proportion of business passengers in total passengers significantly cuts down the total expected revenue (Table 12). Furthermore, the proportion of loyal passengers has a generally positive correlation with the total expected revenue (Table 15).

(4) The experiments on standard benchmark functions demonstrate the advancement of the proposed SFS-PSO compared to the conventional PSO algorithm under the same conditions.

6.2. Policy Suggestions

Price-makers should formulate the optimal price schemes considering the hybrid choice behavior reflected by the differentiated decision-making processes of heterogeneous passengers. Furthermore, railway enterprises provide diverse train products to cater to each passenger category with varied preferences in segmented markets and improve the service quality to cultivate a larger base of loyal passengers.

6.3. Limitations and Further Directions of Research

This study models the choice behaviors of loyal passengers and non-loyal passengers to capture their heterogeneous travel preferences. However, the real market obviously consists of a wider variety of segments where more typical choice behaviors and preferences can be discovered. How to identify distinct passenger choice behaviors to develop

nuanced passenger classifications based on collecting more microscopic data of individual passengers in the further study will be the primary task. On the other hand, due to data limitations, the arrival probability distribution of different passenger categories during the pre-sale period is simplified. In reality, the temporal arrival sequences and arrival probabilities of passengers critically determine whether loyal passengers are able to purchase their preferred train services, significantly impacting both the ticketing process and total expected revenue. Therefore, this research is continued by leveraging intelligent ticket booking systems to capture real-time passenger arrival data which will improve the precision and robustness of the proposed model.

Author Contributions: Conceptualization, Y.W.; methodology, Y.W.; software, Z.W.; data curation, Y.W.; writing—original draft, Y.W.; writing—review and editing, Z.W.; funding acquisition, Z.W. All authors have read and agreed to the published version of the manuscript.

Funding: This research was funded by The National Natural Science Foundation of China, grant number U2468224, and The National Natural Science Foundation of China, grant number U2368212.

Data Availability Statement: The original contributions presented in this study are included in the article. Further inquiries can be directed to the corresponding author.

Conflicts of Interest: Author Yu Wang and Zhendong Wang were employed by the China Academy of Railway Sciences Corporation Limited.

References

1. Guan, X.Y.; Mao, C.H.; Zhou, W.L. A Literature Review of Railway Pricing Based on Revenue Management. *Mathematics* **2023**, *11*, 857. [CrossRef]
2. Li, S.M.; Wong, F.C.L. The effectiveness of differential pricing on route choice. *Transportation* **1994**, *21*, 307–324. [CrossRef]
3. Hu, Z.; Wei, Y.; Xu, Y.; Wang, H.; Li, Y. Optimization of ticket pricing for high-speed railway considering full competitive environment. *Meas. Control.* **2024**, *57*, 1358–1369. [CrossRef]
4. Cao, J.R.; Liu, Z.J.X.; He, Z.H.; Tong, L.; Nie, L. Comprehensive optimization of dynamic pricing and passenger flow assignment for differentiated high-speed train products. *Transp. Policy* **2025**, *165*, 107–126. [CrossRef]
5. Qin, J.; Xu, W.X.; Wu, X.K.; Zeng, Y. Differential Pricing Strategies of High Speed Railway Based on Prospect Theory: An Empirical Study from China. *Sustainability* **2019**, *11*, 3804. [CrossRef]
6. Shi, X.; Zhou, W.L.; Li, X. Optimization of Line Planning by Integrating Ticket Pricing and Seat Allocation Decisions for High-Speed Railway. *Mathematics* **2025**, *13*, 1073. [CrossRef]
7. Jing, Y.; Guo, S.Y.; Chen, F.Q.; Wang, X.; Li, K. Dynamic Differential Pricing of High-Speed Railway Based on Improved GBDT Train Classification and Bootstrap Time Node Determination. *IEEE Trans. Intell. Transp. Syst.* **2022**, *23*, 16854–16866. [CrossRef]
8. Zhang, Q.S.; Qi, J.; Ma, Y.T.; Zhao, J.; Fang, J. Time Differential Pricing Model of Urban Rail Transmit Considering Passenger Exchange Coefficient. *Promet-Traffic Transp.* **2022**, *34*, 609–618. [CrossRef]
9. Yang, Y.; Zhang, X.Q.; Gao, D.S.; Xu, X.; Zheng, B. Research on Choice Preference of Parallel Trains for High-Speed Rail Heterogeneous Passengers. *Transp. Res. Rec.* **2024**, *2678*, 841–854. [CrossRef]
10. Chen, P.F.; Zhang, X.Q.; Gao, D.S. Preference heterogeneity analysis on train choice behaviour of high-speed railway passengers: A case study in China. *Transp. Res. Part A-Policy Pract.* **2024**, *188*, 104198. [CrossRef]
11. Worcester, R.M.; Downham, J.; Nostrand, V. Consumer market research handbook. *J. R. Stat. Soc.* **1972**, *24*, 231.
12. Jian-ming, C.A.I.; Shan, O. Dynamic Differential Pricing of High-speed Railway Parallel Trains Considering Revenue Management. *J. Transp. Syst. Eng. Inf. Technol.* **2020**, *20*, 1–8.
13. Feng, Y.Q.; Li, X.M.; Li, X.W. Rough set theory based travel decision-making factor analysis and weight calculation for railway passengers of compound attribute. *J. China Railw. Soc.* **2014**, *9*, 1–9.
14. Li, Y.; Zhu, H.; Liu, Y. The market segmentation on passenger transportation of High-speed Railway with logistic regression model. In Proceedings of the 2016 International Conference on Logistics, Informatics and Service Sciences (LISS), Sydney, Australia, 24 July 2016; IEEE: New York, NY, USA, 2016; pp. 556–560.
15. Zhang, X.; Lang, M.; Jin, Z. Dynamic pricing for passenger groups of high-speed rail transportation. *J. Rail Transp. Plan. Manag.* **2017**, *6*, 346–356. [CrossRef]
16. Wang, Y.; Zhu, J. Pricing Analysis for Railway Multi-Ride Tickets: An Optimization Approach for Uncertain Demand within an Agreed Time Limit. *Mathematics* **2023**, *11*, 4818. [CrossRef]

17. Ke, Q.; Peng, Z.; Jia-xing, W.E.N. Passenger market segmentation of high-speed railway based on latent class model. *J. Transp. Syst. Eng. Inf. Technol.* **2017**, *17*, 28–34.
18. Su, M.; Luan, W.; Sun, T. Effect of high-speed rail competition on airlines' intertemporal price strategies. *J. Air Transp. Manag.* **2019**, *80*, 101694. [CrossRef]
19. Yan, Z.Y.; Jian, M.Y.; Li, X.J.; Cao, J. Modelling the passenger choice behaviour of buying high-speed railway tickets. *Promet-Traffic Transp.* **2022**, *34*, 455–465. [CrossRef]
20. Gao, D.S.; Zhang, X.Q.; Yang, Y. An empirical study on train choice preferences of high-speed railway passengers: The case of Nanning-Guangzhou railway and Nanning-Beihai railway. *Transp. Lett.-Int. J. Transp. Res.* **2025**, *17*, 805–815. [CrossRef]
21. Qiu, Y.H.; He, Z.H. A Research on Passenger's Travel Choice Behavior in High-speed Railway Based on Passenger Survey Questionnaire. In Proceedings of the International Conference on Applied Mathematics, Modeling and Simulation (AMMS 2018), Beijing, China, 26–27 August 2018; Volume 305, pp. 277–283.
22. Hetrakul, P.; Cirillo, C. Accommodating taste heterogeneity in railway passenger choice models based on internet booking data. *J. Choice Model.* **2013**, *6*, 1–16. [CrossRef]
23. Wang, Y.; Meng, L.Y.; Wang, Z.D.; Abid, M.M. Pricing for Railway Group Tickets in Revenue Management Increasing Revenue and Attracting New Users. *J. Adv. Transp.* **2025**, *2025*, 5549207. [CrossRef]
24. Molina, M.D.; Molina, B.D.; Perez, D.C.; Campos, V.S. Connecting passenger loyalty to preferences in the urban passenger transport: Trends from an empirical study of taxi vs. VTC services in Spain. *Res. Transp. Bus. Manag.* **2021**, *41*, 100661. [CrossRef]
25. Li, B.; Bai, T.F.; Song, Z.Q.; Chen, A.; Wu, B. Public transportation competitiveness analysis based on current passenger loyalty. *Transp. Res. Part A-Policy Pract.* **2018**, *113*, 213–226. [CrossRef]
26. Gurler, H.E. How does service quality predict loyalty? The serial mediation effects of perceived value and consumer brand identification. *Int. J. Qual. Reliab. Manag.* **2024**, *42*, 920–940. [CrossRef]
27. Erturgut, R.; Gürler, H.E. The Effect of Airline Passengers' Satisfaction on Loyalty: Do Region and Airline Carrier Matter? A Meta-analysis Study. *Transp. Dev. Econ* **2023**, *9*, 11. [CrossRef]
28. Akbari, P.; Mesbah, M.; Bagheri, M. Modeling passenger loyalty in intercity rail services using a generalized ordered logit model. *Public Transp.* **2025**, *17*, 347–366. [CrossRef]
29. Wong, J.Y.; Chung, P.H. Retaining Passenger Loyalty through Data Mining: A Case Study of Taiwanese Airlines. *Transp. J.* **2008**, *47*, 17–29. [CrossRef]
30. Saisrikanta, U.; Sana, G.; Uppalapati, P.J.; Karunasri, A.; Narasimharao, K. A Comparative Study for Predicting Airline Passenger Satisfaction. In *Applications of Computational Intelligence in Management and Mathematics (ICCM 2023)*; Springer Proceedings in Mathematics & Statistics; Springer: Cham, Switzerland, 2023; Volume 492.
31. Chacon, J.; Mason, K.J. An Analysis of the Relationship between Passenger Loyalty and Consumer Buying Behavior for Network and Low-Cost Carriers. *Transp. J.* **2011**, *50*, 271–290. [CrossRef]
32. Gu, Y.; Chen, A.T.Y. Modeling mode choice of customized bus services with loyalty subscription schemes in multi-modal transportation networks. *Transp. Res. Part C-Emerg. Technol.* **2023**, *147*, 104012. [CrossRef]
33. Lu, J.; Yang, Z.Z.; Timmermans, H.; Wang, W. Optimization of airport bus timetable in cultivation period considering passenger dynamic airport choice under conditions of uncertainty. *Transp. Res. Part C-Emerg. Technol.* **2016**, *67*, 15–30. [CrossRef]
34. Zhu, Y.T.; Wang, F.Z.; Lv, X.Y.; Pan, Y. Dynamic Pricing for Railway Tickets with Demand-Shifted Passenger Groups. In Proceedings of the 2014 International Conference on Management Science & Engineering (ICMSE), Helsinki, Finland, 25–27 July 2014; pp. 256–262.
35. Zhang, C.; Tian, Q. Pricing strategy of online distribution of airline tickets considering the customers' loyalty. *J. Manag. Sci. China* **2019**, *22*, 31–39.
36. China National Railway Administration. *Technical Support Report for Railway Passenger Service Quality Questionnaire Survey (Award No. TYMK202027)) [Grant Report]*; China National Railway Administration: Beijing, China, 2021.
37. Wiese, M.; Maree, T.; Taylor, C.R. Sticks and stones: How resistance to negative information helps strong brands thrive. *J. Brand Manag.* **2025**, 1–19. [CrossRef]
38. You, P.S. An efficient computational approach for railway booking problem. *Eur. J. Oper. Res.* **2008**, *185*, 811–824. [CrossRef]
39. Katoch, S.; Chauhan, S.S.; Kumar, V. A review on genetic algorithm: Past, present, and future. *Multimed. Tools Appl.* **2021**, *80*, 8091–8126. [CrossRef]
40. Mirjalili, S. Genetic Algorithm. In *Evolutionary Algorithms and Neural Networks*; Studies in Computational Intelligence; Springer: Cham, Switzerland, 2019; Volume 780. [CrossRef]
41. Eaton, J.; Yang, S.X.; Gongora, M. Ant Colony Optimization for Simulated Dynamic Multi-Objective Railway Junction Rescheduling. *IEEE Trans. Intell. Transp. Syst.* **2017**, *18*, 2980–2992. [CrossRef]
42. Karaboga, D.; Basturk, B. A powerful and efficient algorithm for numerical function optimization: Artificial bee colony (ABC) algorithm. *J. Glob. Optim.* **2007**, *39*, 459–471. [CrossRef]

43. Karaboga, D.; Akay, B. A comparative study of Artificial Bee Colony algorithm. *Appl. Math. Comput.* **2009**, *214*, 108–132. [CrossRef]
44. Wang, Y.; Shan, X.; Wang, H.; Zhang, J.; Lv, X.; Wu, J. Ticket Allocation Optimization of Fuxing Train Based on Overcrowding Control: An Empirical Study from China. *Sustainability* **2022**, *14*, 7055. [CrossRef]
45. Chen, S.W. Quantum-Behaved Particle Swarm Optimization with Weighted Mean Personal Best Position and Adaptive Local Attractor. *Information* **2019**, *10*, 22. [CrossRef]
46. Guo, W.A.; Si, C.Y.; Xue, Y.; Mao, Y.; Wu, Q. A Grouping Particle Swarm Optimizer with Personal-Best-Position Guidance for Large Scale Optimization. *IEEE-ACM Trans. Comput. Biol. Bioinform.* **2018**, *15*, 1904–1915. [CrossRef]
47. Dhabal, S.; Sengupta, S. Efficient Design of High Pass FIR Filter using Quantum-behaved Particle Swarm Optimization with Weighted Mean Best Position. In Proceedings of the 3rd International Conference on Computer, Communication, Control and Information Technology (C3IT), Hooghly, India, 7–8 February 2015.
48. Xia, X.W.; Tang, Y.C.; Wei, B. Dynamic multi-swarm global particle swarm optimization. *Computing* **2020**, *102*, 1587–1626. [CrossRef]
49. Nouaouria, N.; Boukadoum, M. Improved global-best particle swarm optimization algorithm with mixed-attribute data classification capability. *Appl. Soft Comput.* **2014**, *21*, 554–567. [CrossRef]
50. Shin, Y.B.; Kita, E. Search performance improvement of Particle Swarm Optimization by second best particle information. *Appl. Math. Comput.* **2014**, *246*, 346–354. [CrossRef]
51. Karim, A.A.; Isa, N.A.M.; Lim, W.H. Modified Particle Swarm Optimization with Effective Guides. *IEEE Access* **2020**, *8*, 188699–188725. [CrossRef]
52. Jin, M.; Lu, H.Y. A multi-subgroup hierarchical hybrid of genetic algorithm and particle swarm optimization. *Control Theory Appl.* **2013**, *10*, 1231–1238.
53. Jiang, J.G.; Ye, H.; Ma, Y.H. Particle swarm optimization algorithm via sampling strategy. *Control Decis.* **2015**, *30*, 1779–1784.
54. Qu, B.Y.; Liang, J.J.; Suganthan, P.N. Niching particle swarm optimization with local search for multi-modal optimization. *Inf. Sci.* **2012**, *197*, 131–143. [CrossRef]
55. An, Z.W. Study on strategy of market-oriented pricing system of high-speed railway emu with sleeping cars. *Railw. Transp. Econ.* **2016**, *38*, 5–9.
56. Nazar, K.H.; Mohammed, Q.; Abdelwahab, M.E.N.; Farag, M.A.; Mostafa, E.; Seyedali, M.; David, G. Schrödinger optimizer: A quantum duality-driven metaheuristic for stochastic optimization and engineering challenges. *Knowl.-Based Syst.* **2025**, *25*, 114273. [CrossRef]

Disclaimer/Publisher's Note: The statements, opinions and data contained in all publications are solely those of the individual author(s) and contributor(s) and not of MDPI and/or the editor(s). MDPI and/or the editor(s) disclaim responsibility for any injury to people or property resulting from any ideas, methods, instructions or products referred to in the content.